UNITED STATES DEPARTMENT OF THE INTERIOR

GEOLOGICAL SURVEY

Empirical laws of order among rivers, faults and earthquakes

Herbert R. Shaw and Anne E. Gartner[1]

Open-File Report 84-356

[1] U.S. Geological Survey Menlo Park, CA. 94025

CONTENTS PAGE

TABLES PAGE

FIGURES PAGE

ABSTRACT

Methods founded in concepts of self similarity are explored for fault studies relative to self similar laws of order for stream systems. This approach has been applied to the ordering relations for a specific fault system in central Nevada (N. Reese River Valley Scarps) and to general arrays of data for statistical relations between fault numbers and lengths in the conterminous United States and the Los Angeles Area. Comparisons with earthquake magnitude-frequency data are given in terms of relations between fault rupture lengths, fault order, earthquake magnitudes and seismic moments. Insofar as we can determine, the results are entirely consistent with a direct parallel between laws of fault order and laws of stream order, including: (1) Law of Fault Numbers; (2) Law of Fault Lengths; (3) Law of Fault Source Areas; (4) Law of Mechanical Energy Gradients; (5) Law of Mecnanical Energy Flux. These conclusions are underscored by recent advances in self-similar models of earthquake mechanisms stemming from Mandelbrot's (1977) concepts of fractal sets, epitomized in studies by Kagan and Knopoff (1977, 1978, 1980, 1981) and by Andrews (1980,1981).

INTRODUCTION

We recently completed a compilation of statistical data representing fault lengths by age and region within the conterminous United States for movements within the latest 15 million years (Shaw and others, 1981) based on the map compiled by Howard and others (1978); we used analogous data for the Los Angeles area (Ziony and others, 1974) as a comparative set at a much larger map scale (factor of 20X). While doing that study we became impressed by resemblances between our data and data representing relations between numbers and lengths of rivers and streams as derived empirically by Horton (1945) and modified by Strahler (1952). They expressed these relations in terms of what have been called Laws of Stream Ordering, in which there are revealed regular systematic relations among the numerical progressions of length, bifurcation ratios, slopes, and corresponding drainage basin areas in a drainage network.

The purpose of this paper is to draw a parallel between methods for stream ordering and methods for ordering fault data, and to direct the results toward new perspectives concerning the geologic distribution and magnitude ranges for earthquakes in the U.S. We find two specific logarithmic relations between fault order (that is, fault sets representing self similar number sets generated in the same manner as stream orders) and earthquake magnitude relative to fault length, depending on the criteria chosen for correlating magnitudes and lengths.

Overall in the United States, the average length ratio for faulting, calibrated according to stream orders, is $R_L \sim 3$. This means that earthquake magnitude is proportional to faulting order divided by 2 when faulting orders are defined in the same way as stream orders and when magnitude is defined according to regressions on length (Mark, 1977; Mark and Bonilla, 1977); on the other hand, if length is determined from a calibration of length versus magnitude, magnitude and order are nearly the same. These results show that self similarity in faulting networks directly parallels self similarity in drainage networks. We do not, however, have an explanation for the seemingly systematic difference in logarithmic base relative to the distinctions in length-magnitude relations. It may be an artifact of the statistical scatter in the length-magnitude data, but the distinctions are suspiciously systematic (see Figure 14).

Our results suggest a new basis for investigating relations between rupture lengths and earthquake magnitudes, and new insights concerning regional source areas (and, presumably, source volumes) in relation to fault lengths and the flow of earthquake energy (flow of mechanical work) in the earth's crust. We also think this approach offers an opportunity for systematic developments in methods of earthquake forecasting based on concepts of self similar fault branching. We see direct parallels with theoretical studies by Kagan and Knopoff (1981) and Andrews (1980, 1981).

THE HORTON AND STRAHLER METHODS OF STREAM ORDERING

The methods used in counting stream segments by Horton (1945) and Strahler (1952) differ somewhat in regard to the convention for classifying stream segments of similar configuration. Both Horton and Strahler counted "unbranched fingertip tributaries" as order 1. Each successively higher order by the Horton method, however, modifies this relation to invoke a trunk stream that remains of that order from its headwater to the next higher order trunk stream. Two effects of this choice are: (a) there is some subjectivity in choosing which branch is the trunk stream, and (b) the total number of segments is smaller than it would be if the order were always unity for every headwater segment. The different methods are derived and discussed in detail by Shreve (1966); Figure 1 summarizes the alternatives and gives histograms and regressions for total counts of stream segments. Figure 2 gives the respective relations among stream order, numbers, and mean lengths based on the classification in Figure 1A. The bifurcation ratios in Figure 2 range from 3 to 5, with an average of 4.6 given by the slope in Figure 2B(3); see Table 2.

Strahler (1971) summarizes the laws of order for stream systems as follows (our headings):

Law of Stream Numbers;

> There follows from observation a law of stream numbers: The numbers of stream segments of successively lower orders in a given basin tend to form a geometric progression, commencing with a single trunk segment of the highest order and increasing according to a constant bifurcation ratio. For example, given a bifurcation ratio of exactly 3 and a trunk-stream segment of the sixth order, the numbers of segments within the system will be 1, 3, 9, 27, 81, and 243 (page 610).

Law of Stream Lengths;

> The mean length of each order is converted into cumulative mean length, by adding the mean length of each order to the sum of those of lower orders.
>
> Extensive observations of drainage networks show that the cumulative length ratio tends to remain constant within a given drainage system. It is therefore possible to state a law of stream lengths: The cumulative mean lengths of stream segments of successively higher orders tend to form a geometric progression beginning with the cumulative mean length of the first-order segments and increasing according to the (constant) length ratio (page 611[1]).

Law of Basin Areas;

> The mean basin areas of successive stream orders tend to form a geometric series beginning with mean area of the first-order basins and increasing according to a constant area ratio (page 612).

[1]We notice that there is a discrepancy between the cumulative mean lengths and the ratios employed in Table 3 (from Strahler, 1971, Table 34.3, p. 611); the ratios actually tabulated apparently were obtained from the mean lengths rather than the cumulative mean lengths.

Law of Energy Gradients[2/];

On the basis of extensive data on channel slopes, a law of stream slopes has been formulated: The mean slopes of stream segments of successively higher orders in a given basin tend to form an inverse geometric series, decreasing according to a constant slope ratio (page 613).

Law of Energy Flux[3/];

When the mean annual discharge, as calculated from stream gauge records, is plotted against the total area of watershed lying above that gauge, a simple relationship of discharge to basin area is revealed. Although the data are plotted on a double-logarithmic graph, the straight line of best fit is so inclined that the discharge increases in direct proportion to the increase in drainage area. Once the existing relationship has been established for a given watershed, it is possible to make good estimates of the mean annual discharge at any given point on a trunk stream by merely measuring the watershed area lying above that point (page 613; italics added)

The various laws of stream order obviously are systematically interrelated. It is evident that if similar, or even analogous, laws of order exist for faulting networks, the potential increase in our abilities to forecast earthquakes may be substantial. We suggest, therefore, that a comparative anatomy of river drainage and faulting networks be created in as great detail as field data will allow. The present paper introduces the idea and draws some tentative correlations for further developments in the field.

[2]We use this phrase to draw attention to possible analogies with mechanical energy flow in faulting and earthquakes. Gradients are steeper in smaller streams for the same net flow because of higher friction losses. Analogously, for the same net work rate across a control surface, the gradient of stress in faulting decreases from the smaller to larger branches of the system; and, of course, frictional dissipation is higher per unit area on the smaller branches.

[3]This relation is a corollary of the Law of Energy Gradients for steady state systems. That is, if the proportions of stream or fault branches are constant, and there is an areal distribution that maintains a constant net discharge across any section normal to the flow, then that discharge is directly proportional to the total available source area for each segment of stream or fault. This appears to state that the net flux of change in potential energy per unit time is, on the average, constant throughout the system. For faults, this means that the net energy flux recorded by the slip on the largest branches is made available by being "collected" and passed along by all the smaller branches relative to the crustal volume sampled by the system.

COMPARATIVE LENGTH FREQUENCIES, STREAMS AND FAULTS

On first consideration, it would seem that faults ought to represent geometrically different phenomena than stream networks. They involve three-dimensional sets of planes that intersect and offset one another in diverse ways over geologically long periods of time. It is probably for this reason that self-similar patterns of branching networks have not been noticed conspicuously, nor have they been generally sought.

The body of data we have compiled, however, is of such wide scope and generality that the complexities of detailed histories have been overwhelmed by patterns that demonstrate common similarities independent of geologic setting, rock types and styles and orientation of faulting (Shaw and others, 1981; also Raleigh and Evernden, 1981, p. 173-176). This "sameness" is the first principle of comparative anatomy, corresponding to the observations made by Horton (1945) that the law of stream numbers is relatively insensitive to isotropy and rock types. As paraphrased by Shreve (1966, page 18):

> Since 1945 investigators working in many different areas have confirmed this insensitivity, showing that both the geometric-series form and the bifurcation ratio are characterized by considerable independence of the detailed geomorphic processes at work in any particular channel network, which in turn implies very general basic causes.

The way data were obtained in Figures 1 and 2 was to measure every segment of stream in Figure 1A. The distribution is somewhat more coherent for the Strahler convention, as might be expected from the relations described earlier. In Figure 1B and 1C the raw data are plotted without regard to ordering; in Figure 2 all data are plotted in terms of numbers and mean lengths in each order designated by either the Horton or Strahler conventions. Figure 1C is a rough numerical test for ordering based on an assumed form of numerical progression. In this case it is for length intervals ordered proportional to mean length. This basis appears to give more consistent regressions than do specific geometric progressions.

The insensitivity of branching statistics to the nature of the system is so general that there is a resemblance between the statistics of stream numbers and fault numbers. Figures 1 and 2 illustrate regressions of number frequencies versus length for the stream segments treated as raw data measured as we did faults (Shaw and others, 1981) and also ordered according to both the Horton and Strahler conventions. The equations for the raw data (Figure 1B), combining regressions of x on y and y on x, are:

$$\log n = -1.03 - 1.00 \log L \quad \text{(Horton)}$$
$$\log n = -1.63 - 1.39 \log L \quad \text{(Strahler)}$$

and for the ordered data, are:

$$\log n = -0.85 - 1.55 \log L \quad \text{(Horton)}$$
$$\log n = -1.22 - 1.67 \log L \quad \text{(Strahler)}$$

where L is in centimeters at a map scale of 1:5,000,000; all data were converted to this scale for comparison with faulting data for the conterminous United States. Where actual lengths are used in tables or figures they are given in kilometers.

The stream data are expressed as histograms and regressions of length frequencies for comparative purposes. Ideally, we would also like to count the orders for fault segments in the same way as stream segments, but the equivalent continuity of branches and flow directions usually are not obvious in the way they are for stream branching; an example involving a simple fault system is described in detail later (Figures 6, 7, and 8). So usually we are making an indirect comparison. Incidently, this method of portraying the length data illustrates another property of stream statistics in common with faulting statistics, and that is the falloff in numbers at the shortest lengths and failure of the power law at the longest lengths. This is an important feature of the data relative to map scale and self similarity; we will return to it later (see Shaw and others, 1981; Kagan and Knopoff, 1981).

Figure 3 gives analogous length distributions for faults in the California Coast Region from Shaw and others (1981; map, Figure 1.-1 (A) and (B); data, Figure 2.1.-1(2), Figure 2.2.1-3.(2)). Figure 4 shows an outline map of faulting regions, and Table 1 identifies the regions by name according to Howard and others (1978); see this map for patterns in post-Miocene fault distributions across the United States.

The regression equation in Figure 3 for Region 2 faults (California Coast) is:

$$\log n = 0.12 - 1.28 \log L; \text{ Constant } \Delta L$$

$$(\log n = 1.60 - 1.70 \log L; \text{ DELX} \sim X)$$

for L in cm at the scale 1,5,000,000. The equation in parentheses is based on the method of length ordering in Figure 1C and described by Shaw and others (1981). Regression equations for other sets of fault data have slope coefficients ranging from about -1 to -2 with a mean of about -1.7, for constant ΔL (Shaw and others, 1981, Tables 2.2.1-1 and 4.2.1-1).

The data set for the California Coast Region in Figure 3 resembles the form of the Strahler distributions of stream lengths in Figure 1B and 1C. Analogous distributions for the thirty Faulting Regions of Table 1, for the conterminous United States overall, and for the Los Angeles Area are given in Shaw and others (1981; Figures 2.2.1-3 and 4.2.1-1). Figure 5 compares the "All U.S." and "L.A." distributions.

Figure 6 shows a local fault pattern in central Nevada, and Figure 7 shows its non-ordered distributions of lengths in the same manner as the previous data. Figure 8, however, treats the faults as an analog of the stream pattern in Figure 1A. In this case, although we can't truly define the orders by the same criteria as streams, because the sequence of fault movements (mechanical energy flow) is not known in the same sense as stream flow, we have counted faults by imagining this pattern to represent a stream drainage pattern with a northeasterly flow into a 4th order trunk fault. That is, we assumed that an ordering sequence exists for faulting networks because of their statistical similarity to stream networks in terms of length frequency relations. In Figure 6 we guessed which would be trunk streams of different orders and then we counted and compared the results of this assumption for the sets of faulting data and comparable stream data (Hightower Creek); numbers and mean lengths are given in Table 2. The comparison between stream and faulting data is geometrically almost identical in Figure 8 and Table 2, perhaps because the fault system is isolated, has narrowly defined movement ages, has similar area to the Hightower Creek system, and is simple.

FAULTING ORDERS CALIBRATED FROM STREAM ORDERS

Table 3 gives data from Morisawa (1962) for the Allegheny River drainage basin as tabulated by Strahler (1971; Table 34.3, p. 611). Figure 9 shows a regression for length orders plotted in a manner corresponding to the stream and fault data in Figure 8; the equation for number versus length is:

$$\log n = 0.22 - 1.48 \log L$$

for L given in cm at 1:5,000,000. We note that the geometric scale, length ranges and slope of the regression equation for the Allegheny network are comparable to data for regional faulting systems (Shaw and others, 1981; Table 4.2.1.-1, p. 262).

Inspection of Tables 2 and 3 and Figures 8 and 9 reveals an interesting relation between length ratio, bifurcation ratio and order. The mean length ratio in Tables 2 and 3 is 3.0 and the mean bifurcation ratios are about 5 for the stream and Reese River fault systems. The absolute slope of the regression line in Figure 7 (N. Reese River faults) is 1.48 (as it is also for the Allegheny River system) and the product with the log of the length ratio is 0.706, giving as antilog the value of the bifurcation ratio 5.08. That is, the product of the slope of the plot of log length frequency times the log of the length ratio determines the log of the bifurcation ratio in ordered sets of either streams or faults. Conversely, given the bifurcation ratio and length ratio, the slope of the plot of log length frequency is determined. Thus, if the mean absolute slope for faulting regions in the United States is 1.70 (constant ΔL basis) and we assume that the length ratio is 3, then the log of the bifurcation ratio is 0.82 and the mean bifurcation ratio is about 6.5. This value is at the upper end of the ranges of bifurcation ratios for stream networks (Shreve, 1966, Figure 3, p. 22). According to Woldenberg (1971) bifurcation ratios in drainage networks generally are mixed, with values ranging from 3 to 7; the largest expected bifurcation ratio for stable drainage systems is 7, but larger ratios may exist in unstable or transiently growing systems.

The above proportionalities are useful, but the systems of ordering are relative. That is, we need to know or assume something about order and one of the values R_b (bifurcation ratio), R_L (length ratio) or S (absolute slope of log length distribution) to determine the other ratios. For fault systems, usually all we know are the length frequencies and S, although we might attempt systems of ordering in special cases as we did in Figure 6, or we might use the DELX~X relation or mixed geometric progressions as a guide (Woldenberg, 1971).

Table 3 gives the data for faulting in the United States assuming a scale similar to the Allegheny drainage system; the table compares numbers, bifurcation, and length ratios between the two systems and gives area ratios based on the Allegheny relations. Figure 10 gives plots for the logarithms of lengths and numbers versus faulting order for "All U.S." and "L.A." data on the basis of the correlations in Table 3. Points are marked on the correlation line for (a) the longest measured fault, (b) the fault length at n=1, (c) the fault length at the maximum frequency, and (d) the shortest measured fault length; these points are indicated for both the constant ΔL and DELX~X conventions.

According to this tentative correlation scheme, the Los Angeles area is a 6th to 8th order faulting system, depending on constant ΔL or DELX conventions, with a cutoff at 3rd order faults reflecting the minimum lengths that were portrayed on the original map scale at 1:250,000. The overall system for the conterminous United States is 8th or 9th order with a cutoff at 3rd or 4th order because of the cutoff on faults portrayed at the map scale 1:5,000,000. This correlation is analogous to measuring the Mississippi River drainage system at 1:5,000,000; tributaries of the first few orders would be poorly represented on this scale.

CORRELATIONS OF FAULT RUPTURE LENGTHS AND EARTHQUAKE MAGNITUDES

Correlations of fault rupture length and earthquake magnitude are discussed by many authors. For consistency, we refer only to the regressions determined by Mark (1977) and Mark and Bonilla (1977) because that method was the basis used in Shaw and others (1981). Figure 11 gives correlations for: (a) strike-slip faults of North America; (b) all faults of North America regardless of type; and (c) all faults of the world regardless of type. Regression equations represent both magnitude on length, and length on magnitude; see discussion by Mark (1977).

Figure 12 identifies the possible relations between order, length, and magnitude using the Allegheny River system as reference. The steeper set of lines in Figure 12A was obtained by calculating magnitude from length calibrated according to Allegheny stream orders in Figure 9. The set of lines with slopes near unity was obtained by calculating length from magnitude based on the same length-order calibration (Figure 9).

Figure 12B expresses the same relations in terms of length (log L) versus order (fault order or magnitude, respectively), illustrating the possible paths for calculating orders of magnitude either for earthquake intensity or rupture length at the same number order. It is interesting that the relations between order and earthquake magnitude are nearly 1:1 when rupture length is calculated according to Mark's regression equations for length on magnitude, while regressions of magnitude on length are steeper by a factor of about 2. This suggests that when dealing with rupture lengths based on earthquake magnitude the ordering progression for length frequencies is a geometric series with base roughly 10 (approx. the bifurcation ratio) whereas the geometric progression of number orders for magnitude calculated from rupture length is roughly to the base 3. The latter is near the lower limit for stream systems and for the N. Reese River Fault Scarps (Figures 8 and 9; Tables 2 and 3), suggesting that it applies to fault systems that are susceptible to ordering according to the Horton-Strahler technique. The former relation can be applied when the ordering classification has not been deciphered from the map pattern, as in the bulk of data for faulting regions in the United States (Shaw and others, 1981).

Figure 13 illustrates the situation where lengths are calculated based only on earthquake counts without any map data for related faulting, demonstrating the base 10 geometric progression (see numerical data in Table 4).

EARTHQUAKE MAGNITUDE-ENERGY-MOMENT RELATIONS

Table 4 gives earthquake energy and seismic moment calculations for some of the data described above, using three different methods of calculating seismic moment. The data are used to introduce concepts of mechanical energy flow analogous to stream flow. The column headed "Event Moment for Constant Total Movement" identifies sets of data based on the assumption of steady state flow; that is, the moment per event times the number of events is constant for all events. Furthermore, it is noticed that these values normalized in terms of the drainage basin area ratios in Table 3 also may be roughly constant as shown in Table 5, suggesting a parallel with the ordering relations of stream flow.

Figure 14 illustrates the calculations of seismic moment in terms of the attenuation factor concept introduced by Evernden (1975). The variety of slopes reflect the different bases for calculating moments, although the general distributions appear to be consistent with the conclusions discussed by Raleigh and Evernden (1981). They also observe that the patterns of behavior from region to region are broadly independent of geologic parameters. Generally speaking, the systems based on earthquake counts (A and D in Table 4) diverge from the control lines, whereas systems based on length frequencies (B and C) are subparallel. Comparison for different regions of the United States is possible based on data in Shaw and others (1981) and is beyond the scope of this paper. There does, however, appear to be some sort of discrepancy between length-magnitude relations and length-moment relations which might be attributed to systematic variatons in the length-magnitude correlations or to attenuation factors varying with length and magnitude.

CONCLUSIONS

We tentatively conclude that fault systems represent self similar branching networks directly analogous to stream drainage systems. So far as can be ascertained on the basis of available data, the correlations are virtually identical in terms of progressions for numbers, lengths, bifurcation and length ratios, and probably even source area (volume) ratios. In turn this suggests that in mature systems, mechanical energy flows at quasi-steady rates with distributions determined by the geometric progressions of branching relations. This conclusion, in turn, suggests some specific relations for maximum earthquake magnitudes, recurrence frequencies, and growth rates of faults in the conterminous United States. These relations are described in companion papers (see Shaw and others, 1981; Shaw and Gartner, 1981; Shaw and Gartner, in press).

Optimally we can look forward to a time when it will be possible to paraphrase seismically the hydrologic law of stream flow in a manner that may resemble the following: "it is possible to make good estimates of the mean annual frequencies and magnitudes of earthquakes at any point on a trunk fault by merely measuring the source area lying above that point in terms of an established fault branching hierarchy and seismic moment flux."

We note that a step in this direction is represented by the synthetic earthquake catalogs generated by Kagan and Knopoff (1981). In fact, it seems that their self similar model for an earthquake catalog is a short term version of our model for fault branching relations. For example, in our Table 4, the "constant moment" models imply that a large earthquake is equivalent to a summation of moments growing from a number of smaller ones (clusters) given by the self similar branching model. In the words of Kagan and Knopoff (1981) the analogous statements for earthquakes are as follows:

> (p. 2853) By virtue of the time scale independence of power law functions we may imagine that the source-time function of a single earthquake, composed of a superposition of overlapping individual events, is identical to that of the history of deformation of the earth due to repeated earthquakes over years or even centuries under a suitable change of time scale.
>
> (page 2861) Our model implies that almost all earthquakes are statistically and causally interdependent, a conclusion that contradicts attempts to divide the full catalog of earthquakes, either into sets of independent or main sequence events or into sets of dependent events (aftershocks and foreshocks). If this picture applies even for the strongest earthquakes, and our results in the previous sections and elsewhere seem to confirm this, then all earthquakes occur in superclusters with very long time spans which may exceed the time spans of all the earthquake catalogs we have at our disposal.

We suggest that data on systems of self similar faults represent information on the nesting of clusters of fault movements and on the "geologic catalog" of earthquake recurrence frequencies beyond the historic earthquake catalogs at our disposal.

REFERENCES

Algermissen, S. T., 1969, Seismic risk studies in the United States. World Conference on Earthquake Engineering, 4th, Santiago, Chile, January 13-18, 1969, Proceedings, v. 1, p. 14-27.

Algermissen, S. T., and Perkins, D. M., 1976, A probabilistic estimate of maximum acceleration in rock in the contiguous U. S.: U.S. Geological Survey Open-file Report 76-416, 45 p.

Andrews, D. J., 1980, A stochastic fault model 1. Static case: Journal of Geophysical Research, v. 85, p. 3867-3877.

Andrews, D. J., 1981, A stochastic fault model 2. Time-dependent case: Journal of Geophysical Research, v. 86, p. 10821-10884.

Evernden, J. F., 1975, Seismic intensities, size of earthquakes and related parameters: Bulletin, Seismological Society of America, v. 65, p. 1287-1313.

Horton, R. E., 1945, Erosional development of streams and their drainage basins; hydrophysical approach to quantitative morphology: Geological Society of America Bulletin, v. 56, p. 275-370.

Howard, K. A., 1978, Preliminary map of young faults in the United States as a guide to possible fault activity: U.S. Geological Survey Miscellaneous Field Studies Map MF-916 (Sheet 1 of 2).

Kagan, Y. Y., and Knopoff, L., 1977, Earthquake risk prediction as a stochastic process: Phys. Earth Planet. Inter., v. 14, p. 97-108.

Kagan, Y. Y., and Knopoff, L., 1978, Statistical study of the occurrence of shallow earthquakes, Geophysical Journal of the Royal Astronomical Society, London, v. 55, p. 67-86.

Kagan, Y. Y., and Knopoff, L., 1980a, Spatial distribution of earthquakes: The two-point correlation function: Geophysical Journal of the Royal Astronomical Society, London, v. 62, p. 303-320.

Kagan, Y. Y., and Knopoff, L., 1980b, Dependence of seismicity on depth: Bulletin, Seismological Society of America, v. 70, p. 1811-1822, 1980b.

Kagan, Y. Y., and Knopoff, L., 1981, Stochastic synthesis of earthquake catalogs: Journal of Geophysical Research, v. 86, p. 2853-2852.

Koyanagi, and Endo, E. T., 1971, Hawaiian seismic events during 1969: U.S. Geological Survey Professional Paper 750C, C-158-C164.

Mandelbrot, B. B., 1977, Fractals: San Francisco, W. H. Freeman and Co.

Mark, R. K., 1977, Application of linear statistical models of earthquake magnitude versus fault length in estimating maximum expectable earthquakes: Geology, v. 5, p. 464-466.

Mark, R. K., and Bonilla, M. G., 1977, Regression analysis of earthquake magnitude and surface fault length using the 1970 data of Bonilla and Buchanan: U.S. Geological Survey Open-file Report 77-614, 8 p.

McGarr, A., 1976, Seismic moments and volume changes: Journal of Geophysical Research, v. 81, p. 1487-1494.

Morisawa, M. E., 1962, Quantitative geomorphology of some watersheds in the Appalachian Plateau: Geological Society of America Bulletin, v. 73, p. 1025-1046.

Raleigh, B., and Evernden, J. F., 1981, Case for low deviatoric stress in the lithosphere in mechanical behavior of crustal rocks: American Geophysical Union Geophysical Monograph 24, p. 173-186.

Richter, C. F., 1958, Elementary Seismology: San Francisco, W. H. Freeman, 768 p.

Shaw, H. R., 1980, The fracture mechanisms of magma transport from the mantle to the surface, in Hargraves, R. B. (editor), Physics of Magmatic Process: Princeton, N. J., Princeton University Press, p. 201-264.

Shaw, H. R., and Gartner, A. E., 1981, Statistical data on faulting rates in the United States and deduced seismicity: Geological Society of American, Abstracts, Programs, v. 13, no. 7, p. 552.

Shaw, H. R., Gartner, A. E., and Lusso, F., 1981, Statistical data for movements on young faults of the conterminous United States; Paleoseismic implications and regional earthquake forecasting: U.S. Geological Survey Open-file Report 81-946.

Shreve, R. L., 1966, Statistical law of stream numbers: Journal of Geology, v. 74, p. 17-38.

Strahler, A. N., 1952, Hypsometric (area-altitude) analysis of erosional topography: Geological Society of America Bulletin, v. 63, p. 1117-1142.

Strahler, A. N., 1964, Quantitative geomorphology of drainage basins and channel networks, in Ven Te Chow (editor), Handbook of Applied Hydrology: Compendium of Water Resources Technology: New York, McGraw-Hill, p. 39-76.

Strahler, A. N., 1971, The Earth Sciences: New York, Harper and Row, 824 p.

Wallace, R. E., 1979, Map of young fault scarps related to earthquakes in north central Nevada: U.S. Geological Survey Open-file Map No. 79-1554.

Woldenberg, M. J., 1971, A structural taxonomy of spatial hierarchies, in M. Chisholm, A. E. Frey, and P. Haggett (eds.) Regional Forecasting: Hamden, Conn., Anchor Books, p. 147-175.

Wyss, M., and Brune, J. N., 1968, Seismic moment, stress and source dimensions for earthquakes in the California-Nevada region: Journal of Geophysical Research, v. 73, p. 4687-4694.

Ziony, J. I., Wentworth, C. M., Buchanan-Banks, J. M., and Wagner, H. C., 1974, Preliminary map showing recency of faulting in coastal southern California: U. S. Geological Survey Miscellaneous Field Studies, Map MF-585 (sheets 1 and 2 of 3).

Table 1 Alphabetical list of fault regions for the conterminous United States (from Howard and others, 1978).

Arizona Mountain Belt	[01]
California Coast	[02]
Central Mississippi Valley	[03]
Circum-Gulf	[04]
Eastern Oregon-Western Idaho	[05]
Four Corners	[06]
Grand Canyon	[07]
Gulf Coast	[08]
Mexican Highland	[09]
Mid-Continent	[10]
Northeast	[11]
Northern Rockies	[12]
Oregon-Washington Coast	[13]
Pacific Interior	[14]
Paradox	[15]
Puget-Olympic	[16]
Rio Grande	[17]
Salton Trough	[18]
Snake River Plain	[19]
Sonoran	[20]
Southeast	[21]
Southern Calif. Borderland	[22]
Straits of Florida	[23]
Transverse Ranges-Tehachapi	[24]
Utah-Nevada	[25]
Walker Lane	[26]
Wasatch-Tetons	[27]
Western Mojave	[28]
Western Nevada	[29]
Wyoming	[30]

Brackets give numbers used in Figure 4.

Table 2. Northern Reese River Valley Scarps1/

Fault order	Number of faults	Bifurcation ratio	Mean length	Length ratio
1	82 (94)		0.45 (0.76)	
		3.2 (4.5)		3.1 (1.7)
2	26 (21)		1.4 (1.3)	
		5.2 (4.2)		2.6 (2.2)
3	5 (5)		3.6 (2.9)	
		5.0 (5.0)		3.1 (3.8)
4	1 (1)		11 (11)	
	average	4.5 (4.6)		2.9 (2.6)

1/Measurements made in this report are based on map patterns from Wallace (1979). Numbers in parentheses are measurements of stream lengths in the Hightower Creek drainage network: Order is based on the Strahler convention; lengths of streams were measured in this report from map pattern in Shreve (1966) taken from Horton (1945).

Table 3 Comparison of United States Faulting data with stream data for Allegheny System (from Strahler, 1971).

Order	Map[1] length (cm at 1:5,000,000)	Log map L	Length (km)	Length ratio (km)	Cumulative Length	Cumulative Length ratio	Number for U.S. faults DELX[2] ~x (a)	Number for U.S. faults Constant Δx[2] (b)	Number Allegheny streams[3] (c)	Bifurcation ratios (a)	Bifurcation ratios (b)	Bifurcation ratios (c)	Area of Allegheny Stream basins[4] (km^2)	Area ratio	
1	0.003	-2.53	0.14		0.14		$5x10^7$	$4x10^5$	5966				0.13		
				3.4		4.4				12	8.6	3.9		3.0	
2	0.010	-2.00	0.48		0.63		$4x10^6$	$4x10^4$	1529				0.39		
				2.7		3.1				6.7	5.4	4.0		5.7	
3	0.026	-1.59	1.29		1.92		$6x10^5$	$8x10^3$	378				2.23		
				3.1		3.1				10	7.4	5.7		7.1	
4	0.081	-1.09	4.03		5.94		$6x10^4$	1000	68				15.8		
				2.8		2.9				6.7	6.1	5.3		5.6	
5	0.23	-0.65	11.3		17.2		$9x10^3$	200	13				88.0		
				2.9		2.9				9.0	6.4	4.3		7.1	avg 5.7
6	0.64	-0.19	32.2		49.4		$1x10^3$	29	3				627		
				3.0		2.9				8.0	6.8	3.0			
7	1.91	+0.28	95.3		145		125	4	1				[3,600]		
				3.0		2.9				8.3	6.62				
8	5.62	+0.75	281		426		15	0.7					[20,500]		
				2.8		2.9				15	6.50				
9	15.8	+1.20	792		1218		1						[117,000]		
				3.0		3.0					6.67				
10	47.9	+1.68	2390		3611										

1 Fault lengths are obtained from the Allegheny Reference curve in Figure 9B.
2 Numbers of faults are obtained from the regression equations in Figure 5A and 5B for log number versus log length.
3 From Figure 9C.
4 Areas are from Strahler (1971, Table 34.3, p. 611) converted to km^2.
The areas in brackets are obtained by extrapolating the data at the average ratio of 5.7.

Table 4 Comparison of earthquake and faulting data: magnitude, length, energy, moment.

(1) Length (km)	(2) Magnitude	(3) Number of events	(4) Energy per event (erg)	Total energy all events (erg)	(5) Moment per event (dyne cm) (a)	(b)	(K = 1-1/2) (c)	Length (km)	Total moment for all events (dyne cm) (a)	(b)	(c)	(6) Event moment for constant total moment (dyne cm) (a)	(c)	(7) Yearly release rates in erg/year: Energy	Moment (a)	(b)	(c)
A Earthquakes of conterminous U.S., approximate time span 2000 years (Algermissen, 1969, Figure 4):																	
1.4	3	4.0×10^{6}	2.0×10^{16}	8.0×10^{22}	2.0×10^{21}	1.6×10^{20}	3.2×10^{24}	1.4	8.0×10^{27}	6.4×10^{26}	1.3×10^{31}	8.0×10^{21}	8.0×10^{21}	4.0×10^{19}	4.0×10^{24}	3.2×10^{23}	6.5×10^{27}
3.1	4	3.2×10^{5}	6.3×10^{17}	2.0×10^{23}	3.2×10^{22}	7.9×10^{21}	1.5×10^{25}	3.1	1.0×10^{28}	2.5×10^{27}	4.8×10^{30}	1.0×10^{23}	1.0×10^{23}	1.0×10^{20}	5.1×10^{24}	1.3×10^{24}	2.4×10^{27}
6.9	5	2.5×10^{4}	2.0×10^{19}	5.0×10^{23}	5.0×10^{23}	4.0×10^{23}	6.8×10^{25}	6.9	1.3×10^{28}	1.0×10^{28}	1.7×10^{30}	1.3×10^{24}	1.3×10^{24}	2.5×10^{20}	6.3×10^{24}	5.0×10^{24}	8.5×10^{26}
16	6	2.0×10^{3}	6.3×10^{20}	1.3×10^{24}	7.9×10^{24}	2.0×10^{25}	3.4×10^{26}	16	1.6×10^{28}	4.0×10^{28}	6.8×10^{29}	1.6×10^{25}	1.6×10^{25}	6.3×10^{20}	7.9×10^{24}	2.0×10^{25}	3.4×10^{26}
35	7	1.6×10^{2}	2.0×10^{22}	3.2×10^{24}	1.3×10^{26}	1.0×10^{27}	1.5×10^{27}	35	2.1×10^{28}	1.6×10^{29}	2.4×10^{29}	2.0×10^{26}	2.0×10^{26}	1.6×10^{21}	1.0×10^{25}	8.0×10^{25}	1.2×10^{26}
78	8	13	6.3×10^{23}	8.1×10^{24}	2.0×10^{27}	5.0×10^{28}	7.0×10^{27}	78	2.6×10^{28}	6.5×10^{29}	9.1×10^{28}	2.5×10^{27}	2.5×10^{27}	4.1×10^{21}	1.3×10^{25}	3.3×10^{26}	4.6×10^{25}
174	9	1	2.0×10^{25}	2.0×10^{25}	3.2×10^{28}	2.5×10^{30}	3.2×10^{28}	174	3.2×10^{28}	2.5×10^{30}	3.2×10^{28}	3.2×10^{28}	3.2×10^{28}	1.0×10^{22}	1.6×10^{25}	1.3×10^{27}	1.6×10^{25}
B. Fault data for conterminous U.S., approximate time span(8) 1300 (49,000) years (Shaw et al., 1981, Figure 4.2.1.-18, Table 4.2.1.-1):																	
0.08	4.05	10^{6}	7.5×10^{17}	7.5×10^{23}	3.6×10^{22}	9.7×10^{21}	1.4×10^{22}	.08	3.6×10^{28}	9.7×10^{27}	1.4×10^{28}	1.1×10^{21}	4.9×10^{22}	5.8×10^{20}	2.8×10^{25}	2.0×10^{23}	2.9×10^{23}
(3.7)	(5.84)		(3.6×10^{20})	(3.6×10^{26})	(5.1×10^{24})	(1.1×10^{25})	(2.1×10^{25})	(3.7)	(5.1×10^{30})	(1.1×10^{31})	(2.1×10^{31})	(5.0×10^{21})	(5.3×10^{23})	(7.4×10^{21})	(1.1×10^{26})	(2.2×10^{26})	(4.3×10^{26})
0.32	4.70	10^{5}	7.1×10^{18}	7.1×10^{23}	2.2×10^{23}	1.2×10^{23}	1.9×10^{23}	.32	2.2×10^{28}	1.2×10^{28}	1.9×10^{28}	1.0×10^{22}	4.9×10^{23}	5.5×10^{20}	1.7×10^{25}	2.4×10^{23}	3.9×10^{23}
(9.0)	(6.26)		(1.5×10^{21})	(1.5×10^{26})	(1.6×10^{25})	(5.5×10^{25})	(1.1×10^{26})	(9.0)	(1.6×10^{30})	(5.5×10^{30})	(1.1×10^{31})	(5.0×10^{22})	(5.3×10^{24})	(3.1×10^{21})	(3.3×10^{25})	(1.1×10^{26})	(2.2×10^{26})
1.2	5.30	10^{4}	5.6×10^{19}	5.6×10^{23}	1.2×10^{24}	1.3×10^{24}	2.4×10^{24}	1.2	1.2×10^{30}	1.3×10^{28}	2.4×10^{28}	1.0×10^{23}	4.9×10^{24}	4.3×10^{20}	9.2×10^{24}	2.7×10^{23}	4.9×10^{23}
(22)	(6.68)		(6.6×10^{21})	(6.6×10^{25})	(5.2×10^{25})	(2.9×10^{26})	(6.2×10^{26})	(22)	(5.2×10^{29})	(2.9×10^{30})	(6.2×10^{30})	(5.0×10^{23})	(5.3×10^{25})	(1.4×10^{21})	(1.1×10^{25})	(5.9×10^{25})	(1.3×10^{26})
4.3	5.91	10^{3}	4.6×10^{20}	4.6×10^{23}	6.2×10^{24}	1.4×10^{25}	2.8×10^{25}	4.3	6.2×10^{27}	1.4×10^{28}	2.8×10^{28}	1.0×10^{24}	4.9×10^{25}	3.5×10^{20}	4.8×10^{24}	2.9×10^{23}	5.7×10^{23}
(53)	(7.09)		(2.7×10^{22})	(2.7×10^{25})	(1.6×10^{26})	(1.4×10^{27})	(3.3×10^{27})	(53)	$1.6\times10^{29})$	(1.4×10^{30})	(3.3×10^{30})	(5.0×10^{24})	(5.3×10^{26})	(6.0×10^{20})	(3.3×10^{24})	(2.9×10^{25})	(6.7×10^{25})
16	6.53	10^{2}	3.9×10^{21}	3.9×10^{23}	3.4×10^{25}	1.6×10^{26}	3.4×10^{26}	16	3.4×10^{27}	1.6×10^{28}	3.4×10^{28}	1.0×10^{25}	4.9×10^{26}	3.0×10^{20}	2.6×10^{24}	3.3×10^{23}	7.0×10^{23}
(128)	(7.50)		(1.1×10^{23})	(1.1×10^{25})	(5.0×10^{26})	(7.1×10^{27})	(1.8×10^{28})	(128)	(5.0×10^{28})	(7.1×10^{29})	(1.8×10^{30})	(5.0×10^{25})	(5.3×10^{27})	(2.0×10^{20})	(1.0×10^{24})	(1.4×10^{25})	(3.7×10^{25})
58	7.13	10	3.1×10^{22}	3.1×10^{23}	1.8×10^{26}	1.7×10^{27}	4.0×10^{27}	58	1.8×10^{27}	1.7×10^{28}	4.0×10^{28}	1.0×10^{26}	4.9×10^{27}	2.4×10^{20}	1.4×10^{24}	3.5×10^{23}	8.2×10^{23}
(310)	(7.92)		(4.8×10^{23})	(4.8×10^{24})	(1.6×10^{27})	(3.7×10^{28})	(9.7×10^{28})	(310)	(1.6×10^{28})	(3.7×10^{29})	(9.7×10^{29})	(5.0×10^{27})	(5.3×10^{28})	(1.0×10^{20})	(0.3×10^{24})	(7.6×10^{24})	(2.0×10^{25})
216	7.75	1	3.4×10^{23}	3.0×10^{23}	1.0×10^{27}	1.9×10^{28}	4.9×10^{28}	216	1.0×10^{27}	1.9×10^{28}	4.9×10^{28}	1.0×10^{27}	4.9×10^{28}	2.3×10^{20}	0.8×10^{24}	3.9×10^{23}	1.0×10^{24}
(751)	(8.33)		(2.0×10^{24})	(2.0×10^{24})	(5.0×10^{27})	(1.8×10^{29})	(5.3×10^{29})	(751)	(5.0×10^{27})	(1.8×10^{29})	(5.3×10^{29})	(5.0×10^{27})	(5.3×10^{29})	(0.4×10^{20})	(0.1×10^{24})	(3.7×10^{24})	(1.1×10^{25})
C. Northern Reese River Valley faults, approximate time span 1000 years (Data from this report; based on Wallace, 1979):																	
0.45	4.8	82	1.4×10^{19}	1.2×10^{21}	4.0×10^{23}	2.5×10^{23}	3.7×10^{23}	0.45	3.3×10^{25}	2.1×10^{25}	3.0×10^{25}	3.0×10^{23}	2.1×10^{24}	1.2×10^{18}	3.3×10^{22}	2.1×10^{22}	3.0×10^{22}
1.4	5.4	26	7.9×10^{19}	2.1×10^{21}	1.6×10^{24}	2.0×10^{24}	3.2×10^{24}	1.4	4.2×10^{25}	5.2×10^{25}	8.3×10^{25}	9.6×10^{23}	6.5×10^{24}	2.1×10^{18}	4.2×10^{22}	5.2×10^{22}	8.3×10^{22}
3.6	5.8	5	3.2×10^{20}	1.6×10^{21}	5.0×10^{24}	9.3×10^{24}	2.0×10^{25}	3.6	2.5×10^{25}	4.7×10^{25}	1.0×10^{26}	5.0×10^{24}	3.4×10^{25}	1.6×10^{18}	2.5×10^{22}	4.7×10^{22}	1.0×10^{23}
11	6.4	1	2.5×10^{21}	2.5×10^{21}	2.5×10^{25}	1.0×10^{26}	1.7×10^{26}	11	2.5×10^{25}	1.0×10^{26}	1.7×10^{26}	2.5×10^{25}	1.7×10^{26}	2.5×10^{18}	2.5×10^{22}	1.0×10^{23}	1.7×10^{23}
D. Kilauea earthquakes in 1969, approximate time span 1 year (Shaw, 1980, Table 2):																	
0.52	2	600	6.3×10^{14}	3.8×10^{17}	1.3×10^{20}	3.2×10^{18}	4.9×10^{23}	0.52	0.8×10^{23}	1.9×10^{21}	2.9×10^{26}	3.3×10^{21}	3.0×10^{23}	0.4×10^{18}	0.8×10^{23}	1.9×10^{21}	2.9×10^{26}
1.2	3	60	2.0×10^{16}	1.2×10^{18}	2.0×10^{21}	1.6×10^{20}	2.4×10^{24}	1.2	1.2×10^{23}	9.6×10^{21}	1.4×10^{26}	3.3×10^{21}	3.0×10^{24}	1.2×10^{18}	1.2×10^{23}	9.6×10^{21}	1.4×10^{26}
2.5	4	8	6.3×10^{17}	5.7×10^{18}	3.2×10^{22}	7.9×10^{21}	9.8×10^{24}	25	2.9×10^{23}	7.1×10^{22}	8.8×10^{25}	2.2×10^{23}	2.0×10^{25}	5.7×10^{18}	2.9×10^{23}	7.1×10^{21}	8.8×10^{25}
5.5	5	2	2.0×10^{19}	4.0×10^{19}	5.0×10^{23}	4.0×10^{23}	4.4×10^{25}	5.5	1.0×10^{24}	8.0×10^{23}	8.8×10^{25}	2.0×10^{24}	1.8×10^{26}	4.0×10^{19}	1.0×10^{24}	8.0×10^{23}	8.8×10^{25}

(1) Lengths for the conterminous U. S. were calculated from the recurrence data of Algermissen (1969) using the equation for length based on magnitude for North America according to Mark and Bonilla (1977). The equation is $\log L(km) = -0.91 + 0.35 M$. Lengths for Kilauea are based on data in Shaw (1980, Table 2) using equation for worldwide rupture lengths from Mark and Bonilla (1977): $\log L(km) = -0.96 + 0.34 M$.

(2) Magnitude calculated from Mark and Bonilla (1977) using the equation for magnitude based on length for North America: $M = 5.23 + 1.08 \log (L)$, for L in km.

(3) The numbers of earthquake events are taken directly from the published data base above; fault data are obtained from the length number relation cited in this paper.

(4) Earthquake energy is calculated from the equation (Richter, 1958, p. 366): $\log E = 11.8 + 1.5 M$, where E is the radiated energy in ergs.

(5) Seismic moments (dyne-cm) and total moments (moment times number of events) are obtained, respectively, from the equations: (a) $\log M_0 = 17.7 + 1.2 M$ (McGarr, 1976); (b) $\log M_0 = 15.1 + 1.7 M$ (Wyss and Brune, 1968); (c) $M_0 = 1.91 \log L + 24.23$ (Raleigh and Evernden, 1981, figure 5 for $k = 1$-1/2).

(6) The event moment for constant total moment is obtained by taking the total moment at the highest magnitude and dividing that value by the numbers of events at each successively lower magnitude.

(7) The yearly release rates for energy and moment are obtained by dividing the totals by the respective time spans (see footnote 8) represented by the data. For constant event moment, the rate is the value at largest magnitude.

(8) The time spans are obtained from: A. Recurrence times for the largest earthquakes; B. Total fault rupture lengths divided by fractional rupture length rates based on a total rate of 100 km/yr times the fractions $(nL)/\Sigma nL)$; C. The order of magnitude for the mean movement age; D. The earthquake count period of Koyanagi and Endo (1971).

Table 5 Seismic moment flux for earthquakes of conterminous U.S. based on fault source area drainage basin area analogy.

(1) Order	(2) Basin area (km^2)	(3) Event moment (constant total) (dyne cm)	(4) Event moment/ Basin area (erg/km^2)	(5) Earthquake source Area for constant flux (km^2) (a)	(b)
0 (M=4)	[.03]	1.0×10^{23}	3.3×10^{24}	0.04	1
2 (M=5)	0.39	1.3×10^{24}	3.3×10^{24}	[0.4]	11
4 (M=6)	15.8	1.6×10^{25}	1.0×10^{24}	4.8	130
6 (M=7)	627	2.0×10^{26}	0.32×10^{24}	61	1700
8 (M=8)	[20,400]	2.5×10^{27}	0.12×10^{24}	760	[20,400]
10 (M=9)	[661,000]	3.2×10^{28}	0.05×10^{24}	9700	270,000

(1) Order is estimated from Figure 12 for earthquake magnitudes calculated from length. The values in parentheses are the magnitudes.

(2) Basin areas are from Table 3. Bracketed values are extrapolated according to constant area ratio.

(3) Event moments are from Table 4, column (c).

(4) This is the flux of earthquake moment if the total moment for each fault order is constant. Moment flux equals event moment divided by basin area.

(5) This is the source area required to satisfy both constancy of total moment and constancy of seismic moment flux; i.e., this is the model for uniformly steady energy flow. Column (a) is normalized relative to Order 2 area and column (b) is normalized to Order 8 area shown in brackets. These two area sets span the smallest and largest expected source areas for the indicated orders and earthquake magnitudes.

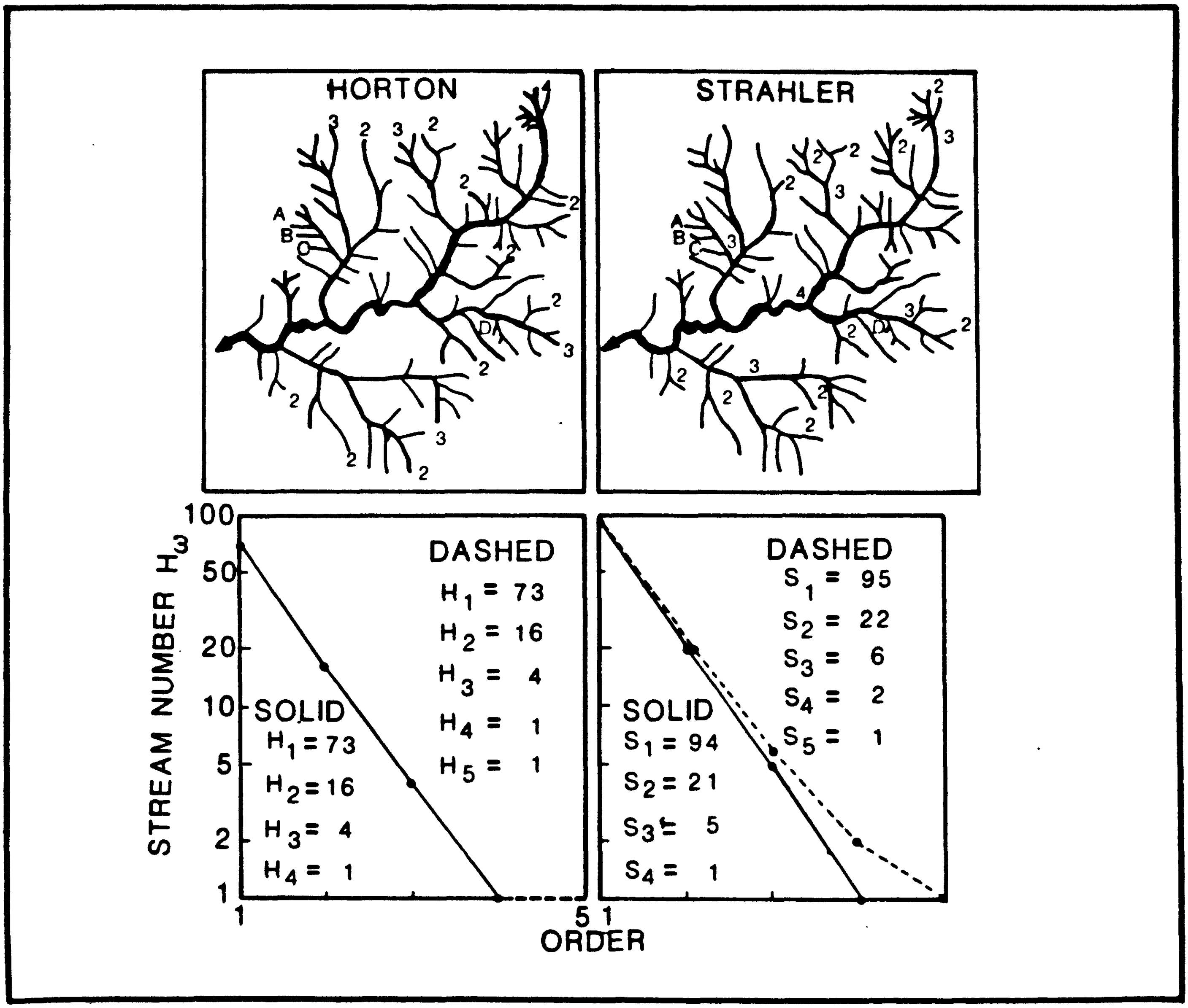

Figure 1. Procedure for determination of stream order in a drainage network according to Horton (1945) and Strahler (1952); data for Hightower Creek, redrawn from Shreve (1966).
A. Numbers on the map indicate the highest order for a branching subsystem; fingertip tributaries are order 1 (see text). The graphs of stream numbers represent the counts for segments in each order; the dashed curve tests an assumption that the system might be 5th order.

STREAM LENGTHS HIGHTOWER CREEK AREA

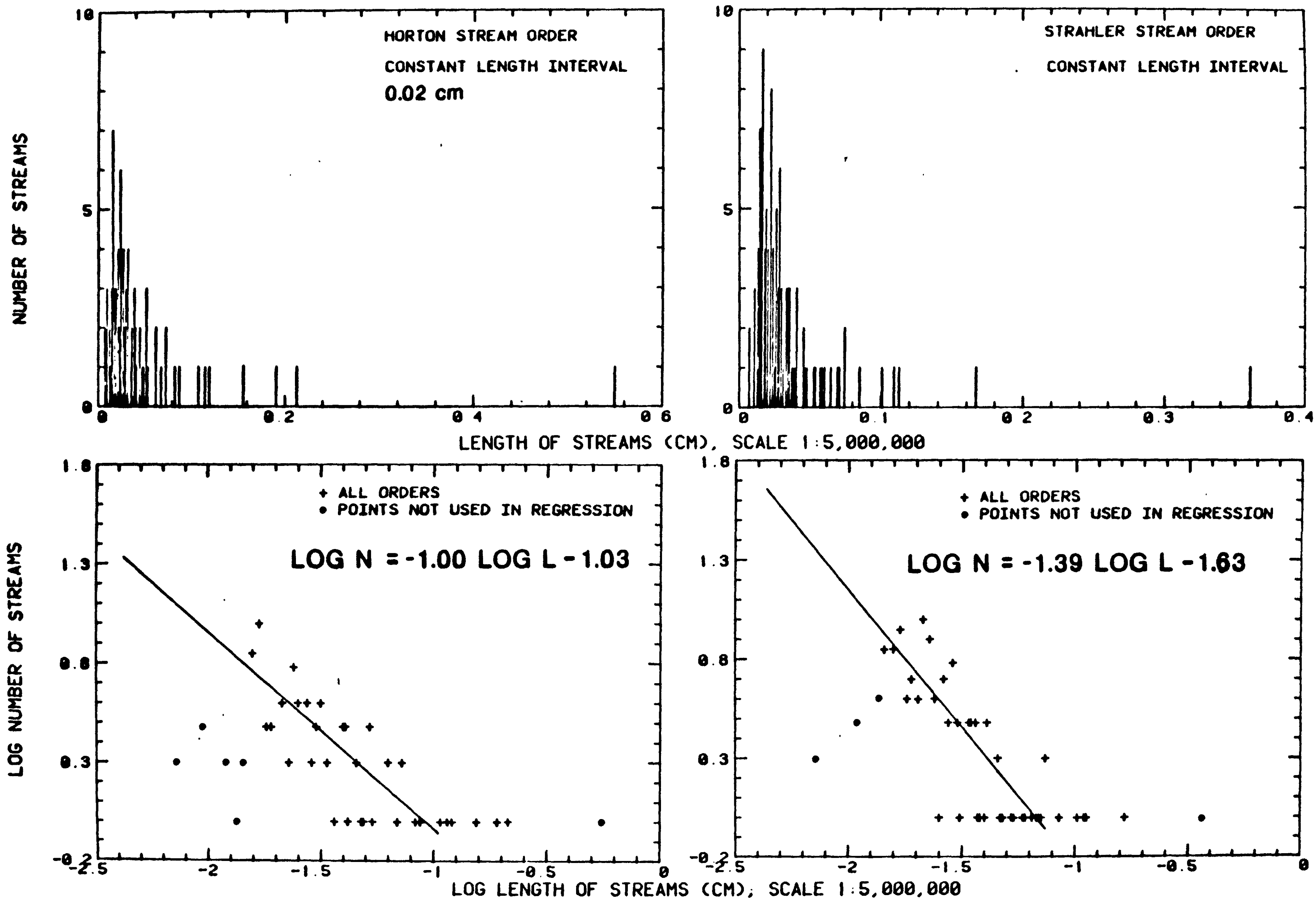

B. Histograms and regressions for the logarithm of number frequencies versus logarithm of length for stream segments measured and counted without regard to order and for constant increments of length.

LENGTH OF STREAMS HIGHTOWER CREEK AREA

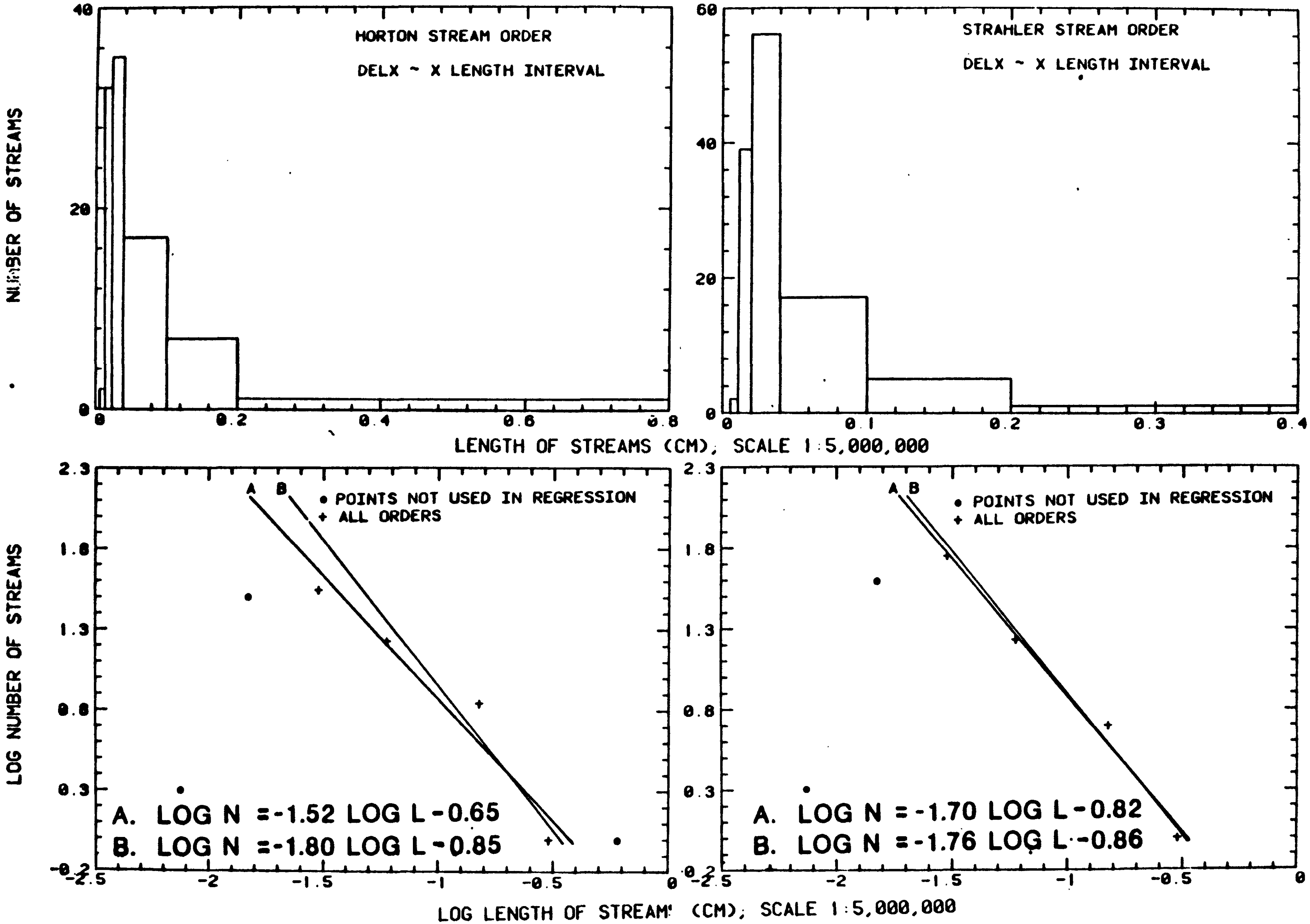

C. Same as B., except that the length intervals are increased according to mean length in the interval; this convention is designated DEL~X. The expanding scale results in inclusion of all the data and an improved regression fit. Curves A and B represent different assumptions about points included in the regression. Geometric progressions to the base 2 and 3 were also tested and gave similar but less precise regressions. This approach offers an alternate way to test for ordering relations when the order can not be determined on the basis of branching patterns.

1C

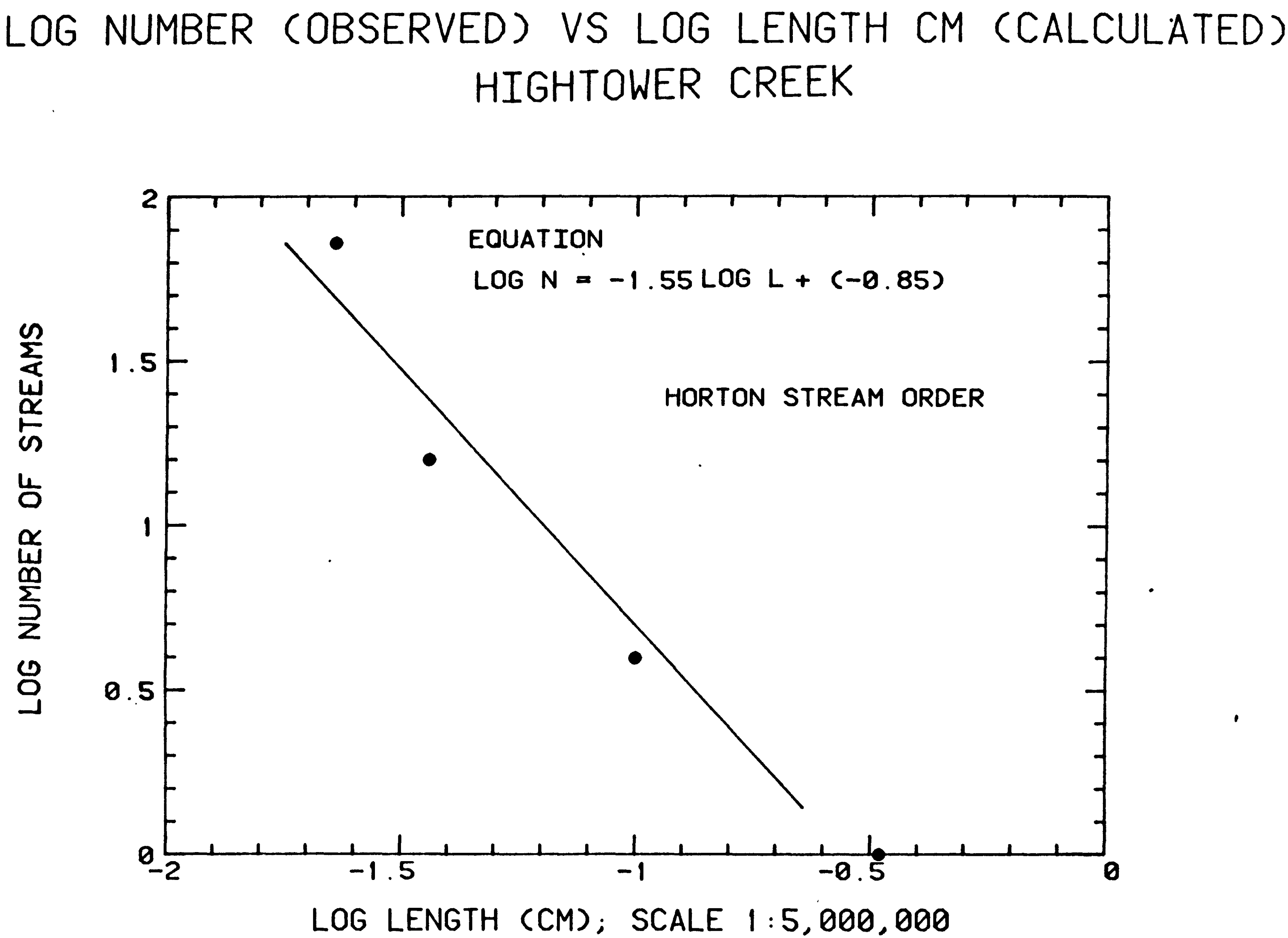

Figure 2. Relationships of order, numbers and mean lengths based on either the Horton or Strahler classifications for Hightower Creek data: A. Horton classification; (1) log number vs log length, (2) log length vs stream order, (3) log number vs stream order.

2A(1)

STREAM ORDER (OBSERVED) VS LOG LENGTH CM (CALCULATED)
HIGHTOWER CREEK

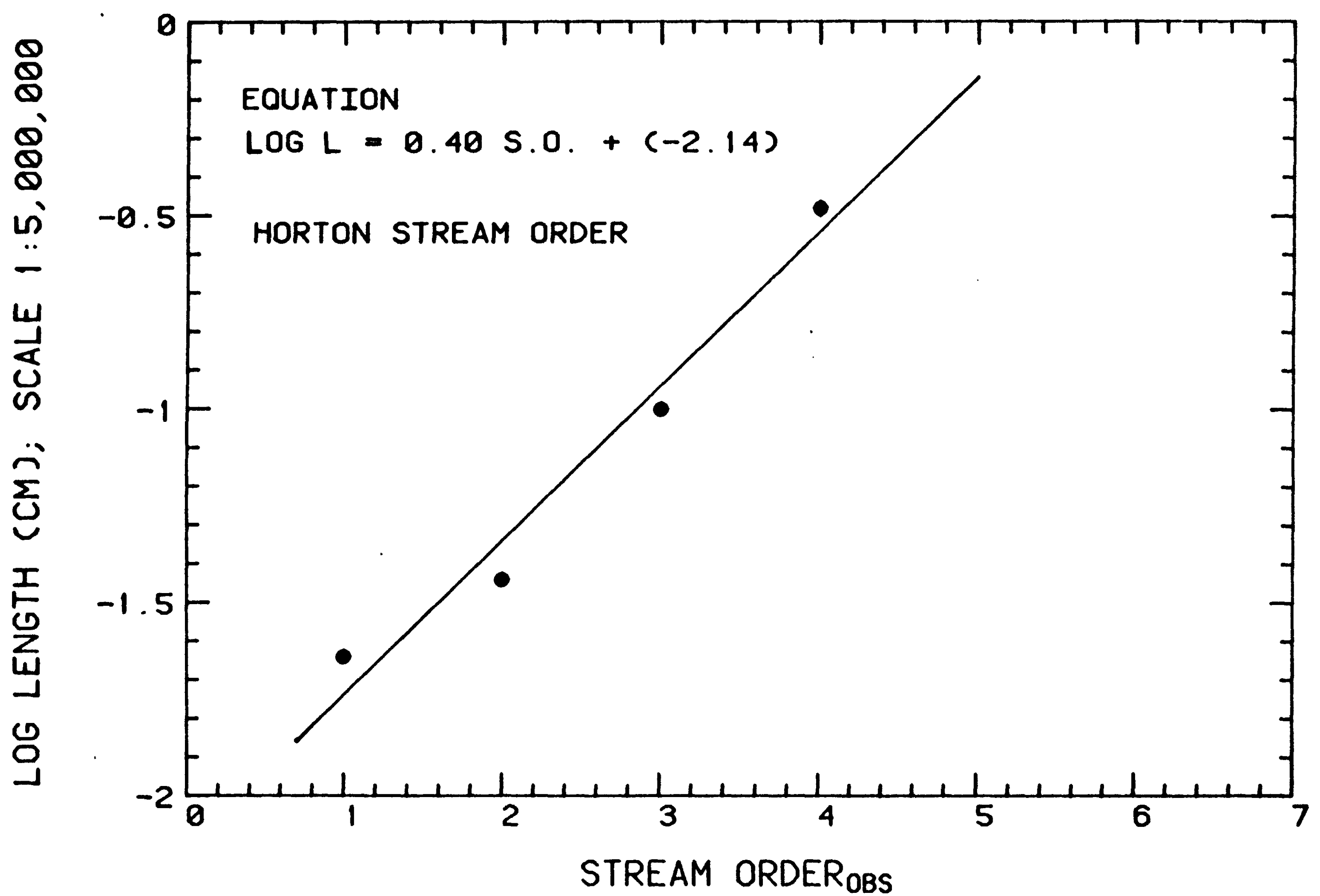

2A(2)

STREAM ORDER (OBSERVED) VS LOG NUMBER (OBSERVED)
HIGHTOWER CREEK

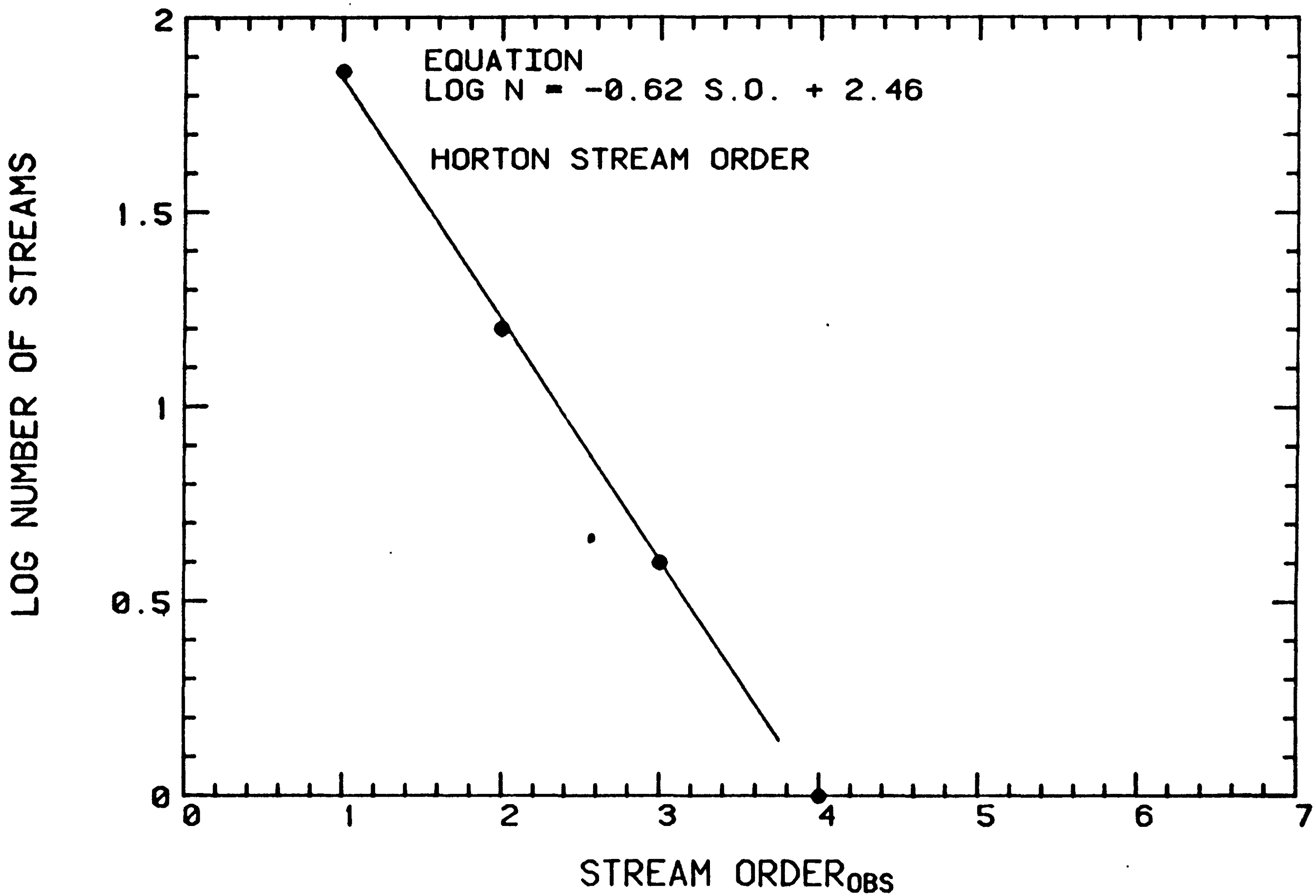

2A(3)

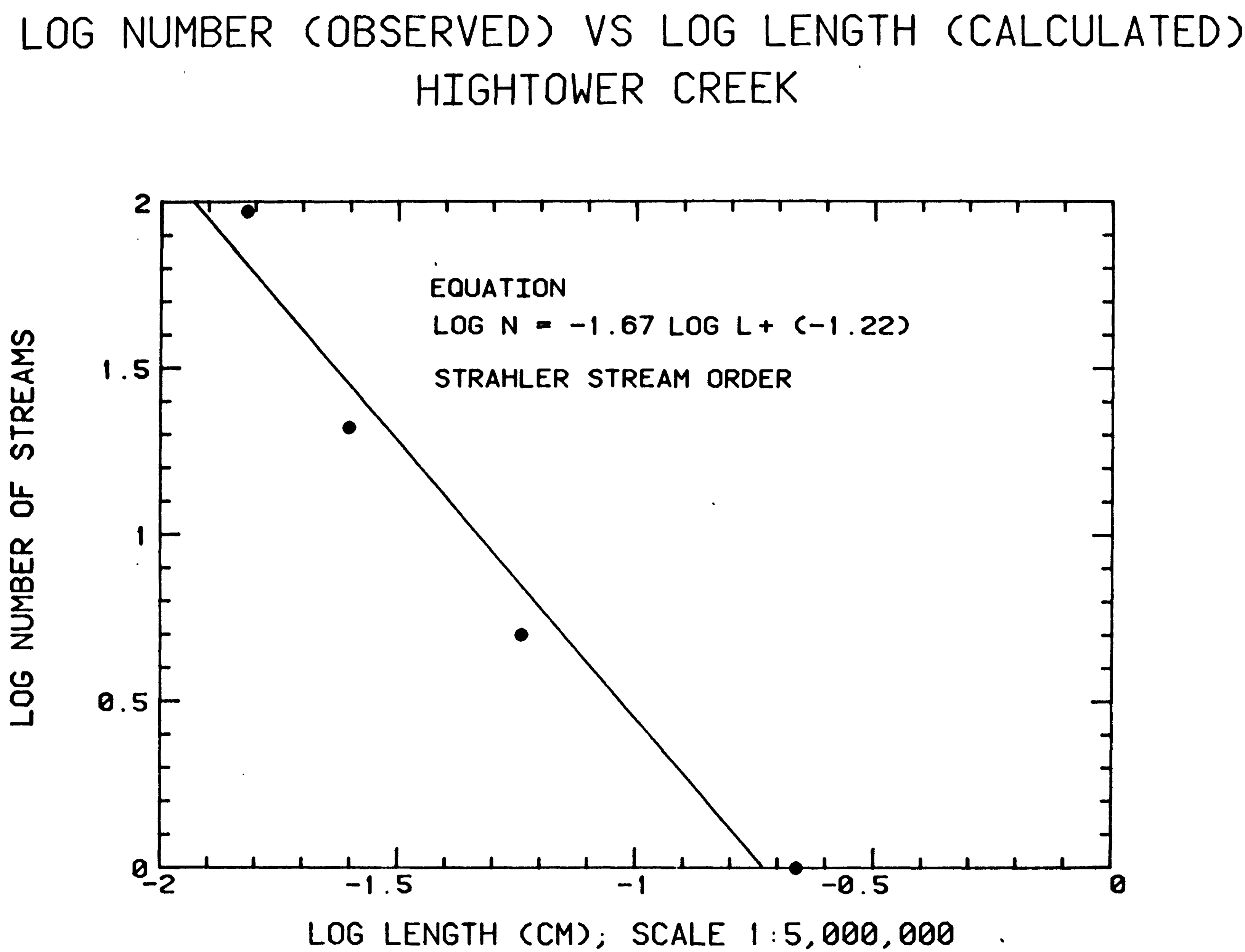

2B(1)

B. Strahler classification; Ditto.

Note: The regression equations for log number vs log length resemble the equations based on the DELX~X convention in Figure 1C, suggesting that it offers an approximate basis for determining branching orders in the absence of clear criteria for classifying order from map patterns.

STREAM ORDER (OBSERVED) VS LOG LENGTH CM (CALCULATED)
HIGHTOWER CREEK

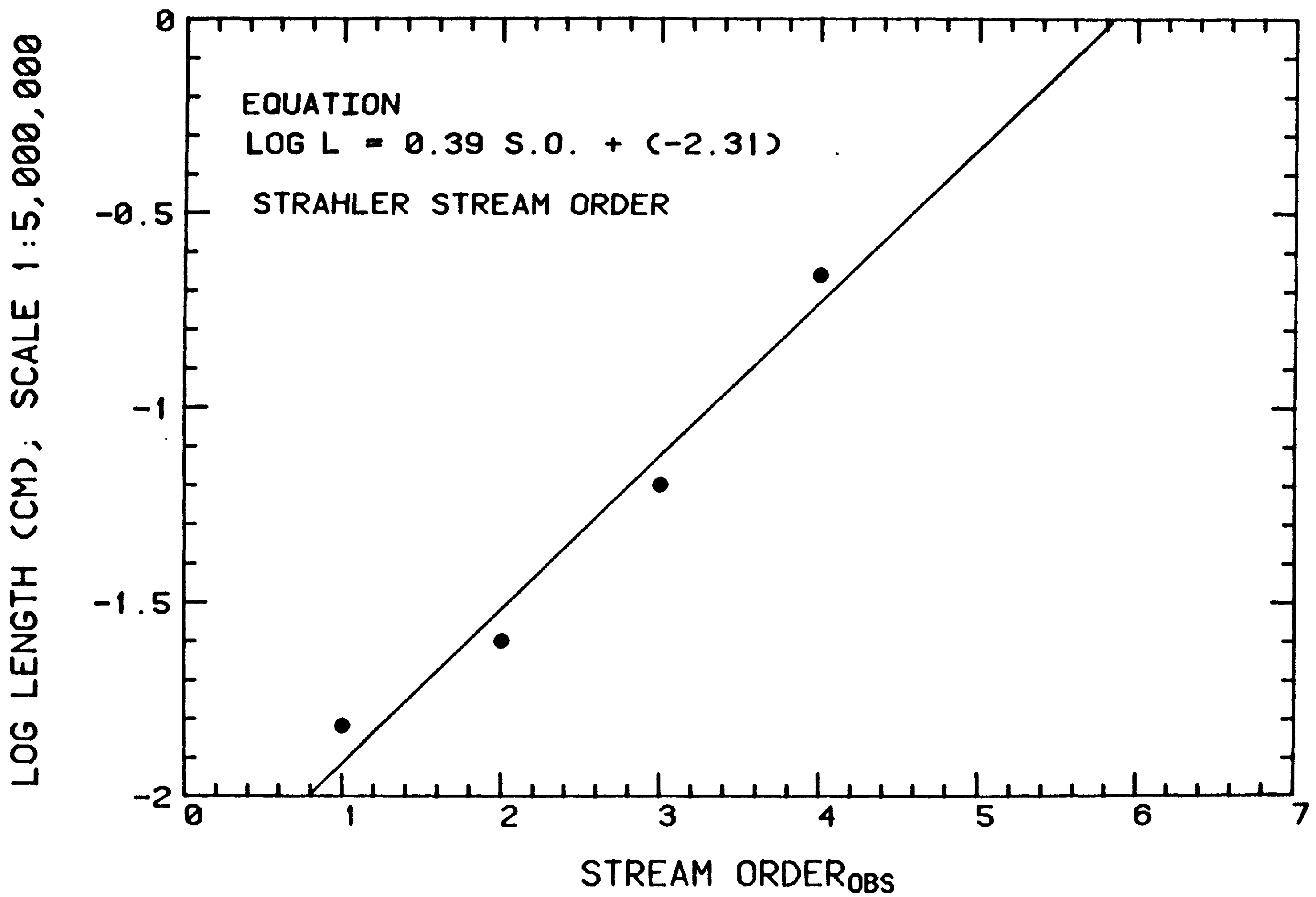

2B(2)

STREAM ORDER (OBSERVED) VS LOG NUMBER (OBSERVED)
HIGHTOWER CREEK

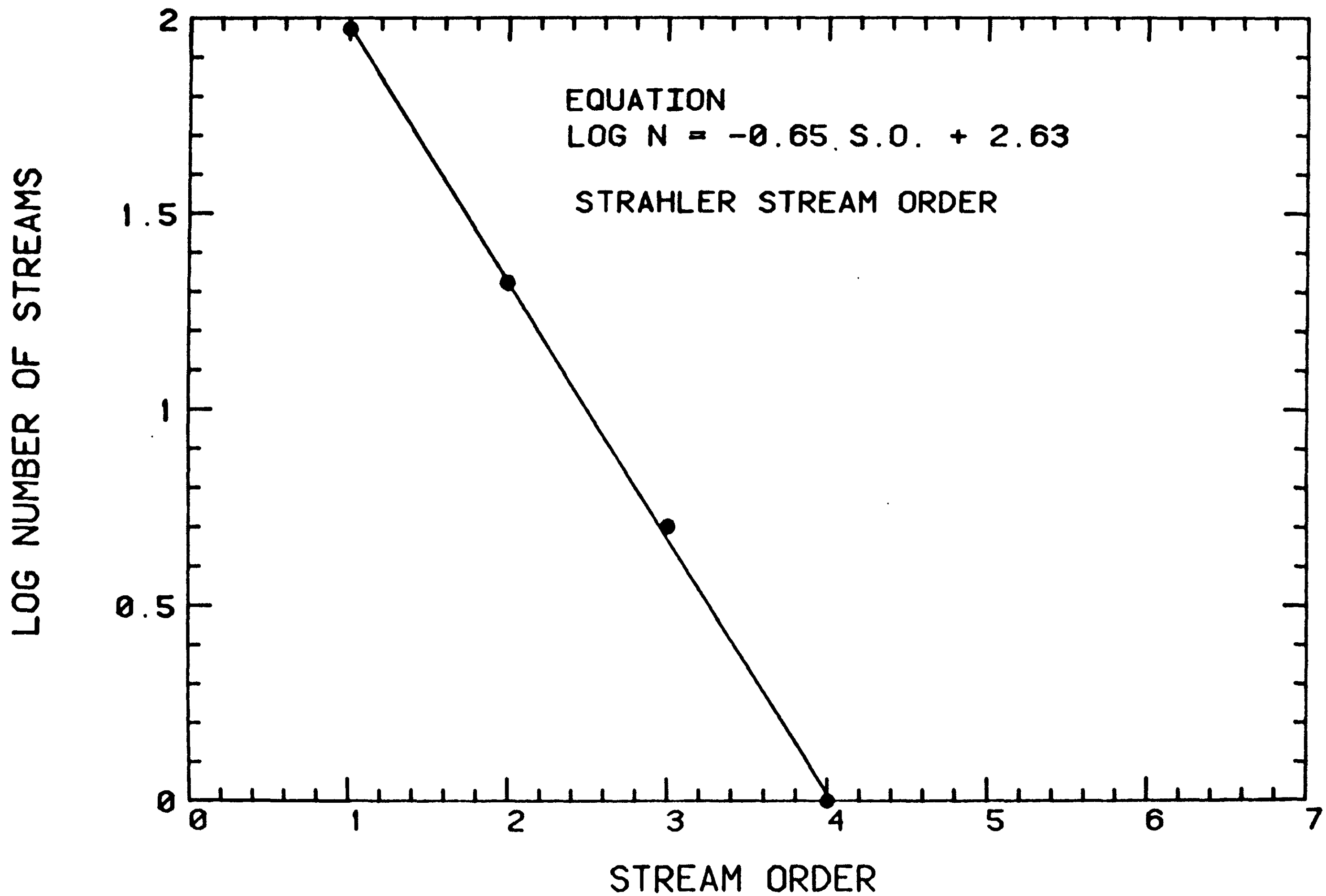

2B(3)

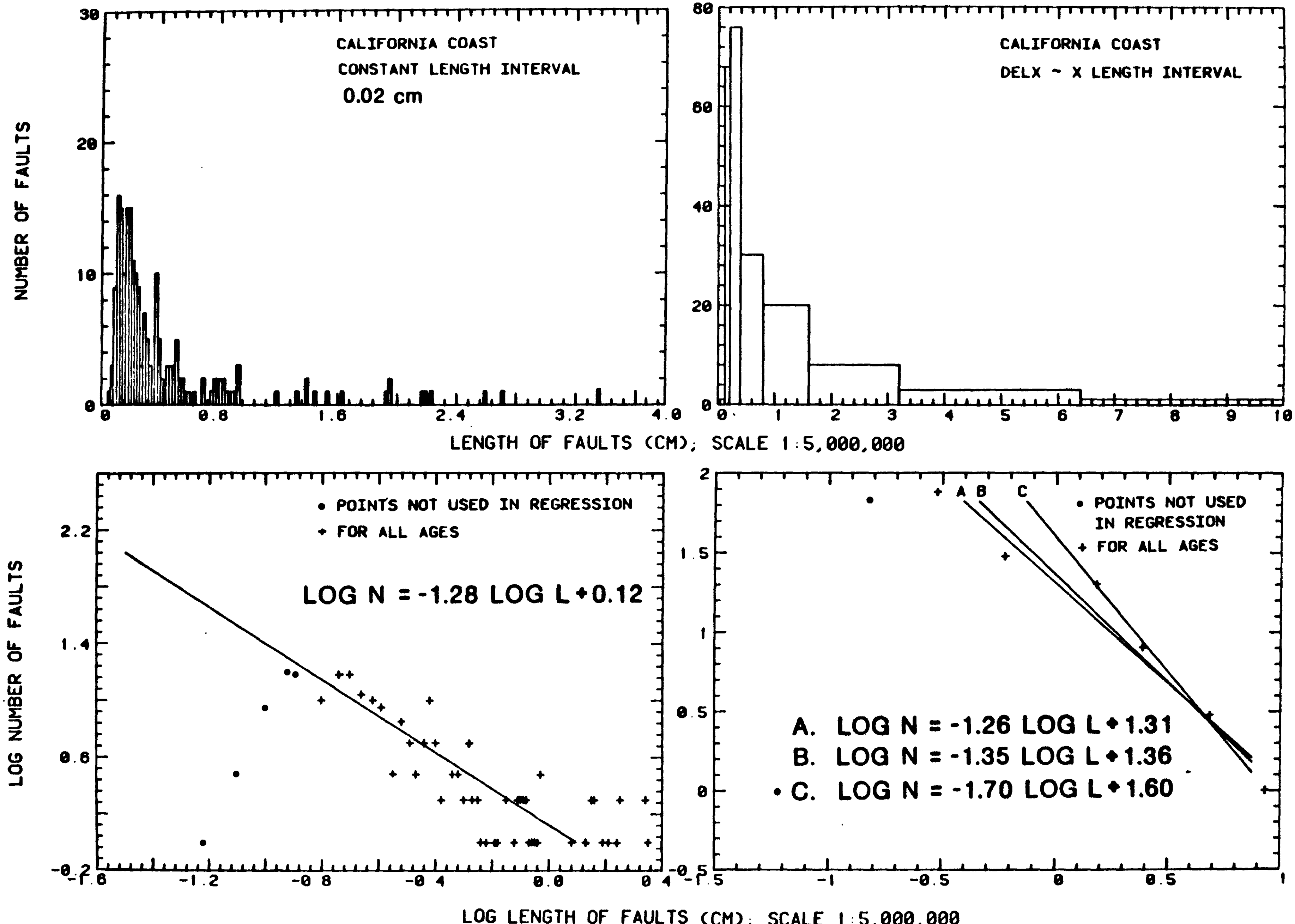

Figure 3. Histograms and regressions for number frequencies versus length for faults of the California Coast Region (Region 2 of Figure 4). The three equations A through C for the DELX X convention result from progressively eliminating data points, left to right, until an essentially constant slope is obtained; data from Shaw and others(1981).

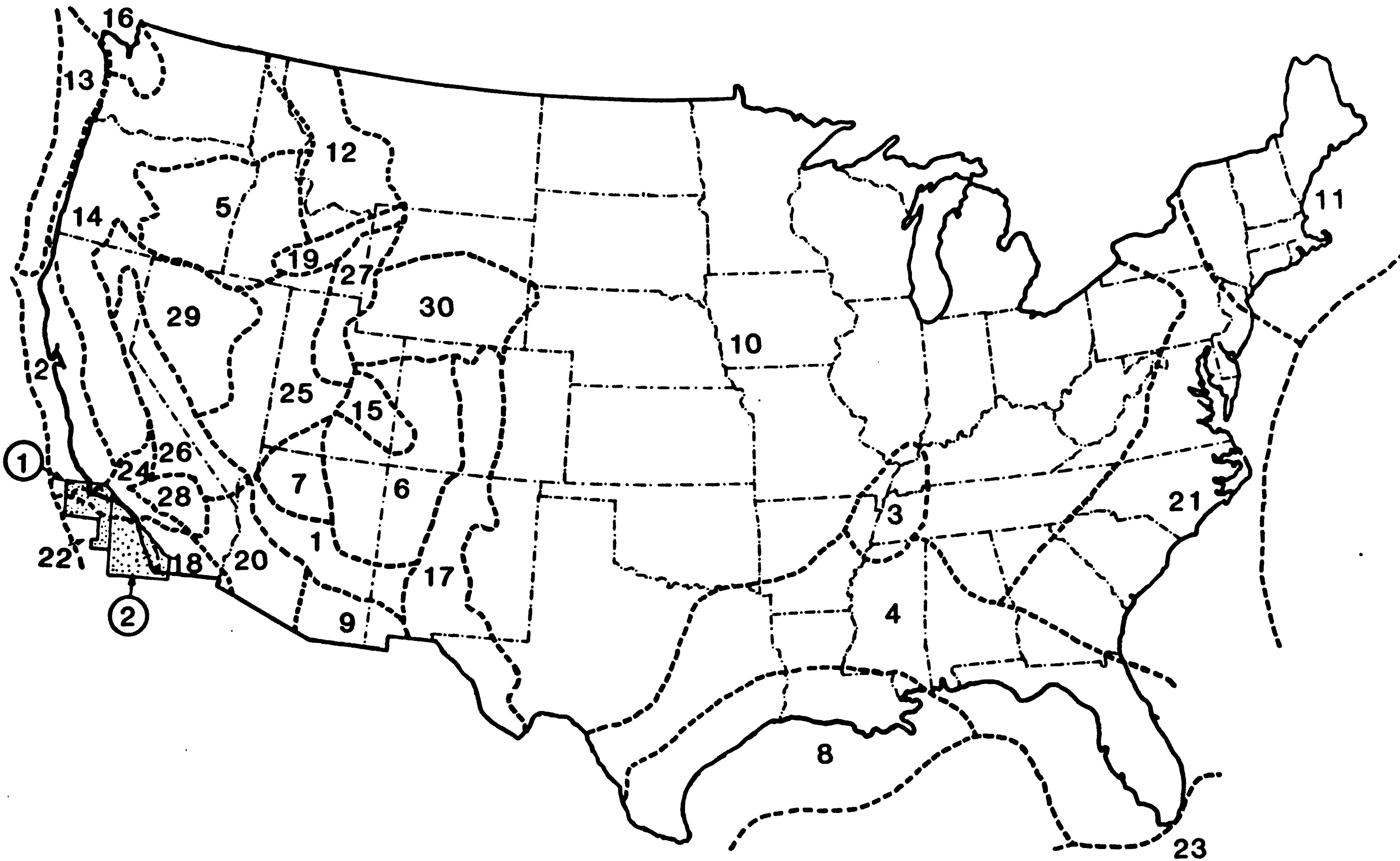

Figure 4. Index map for faulting regions in the conterminous U.S. based on Howard and others (1978), and the Los Angeles area, based on Ziony and others (1974). Numbered regions are identified by name in Table 1. The stippled areas numbered 1 and 2 represent the maps for the Los Angeles area.

4

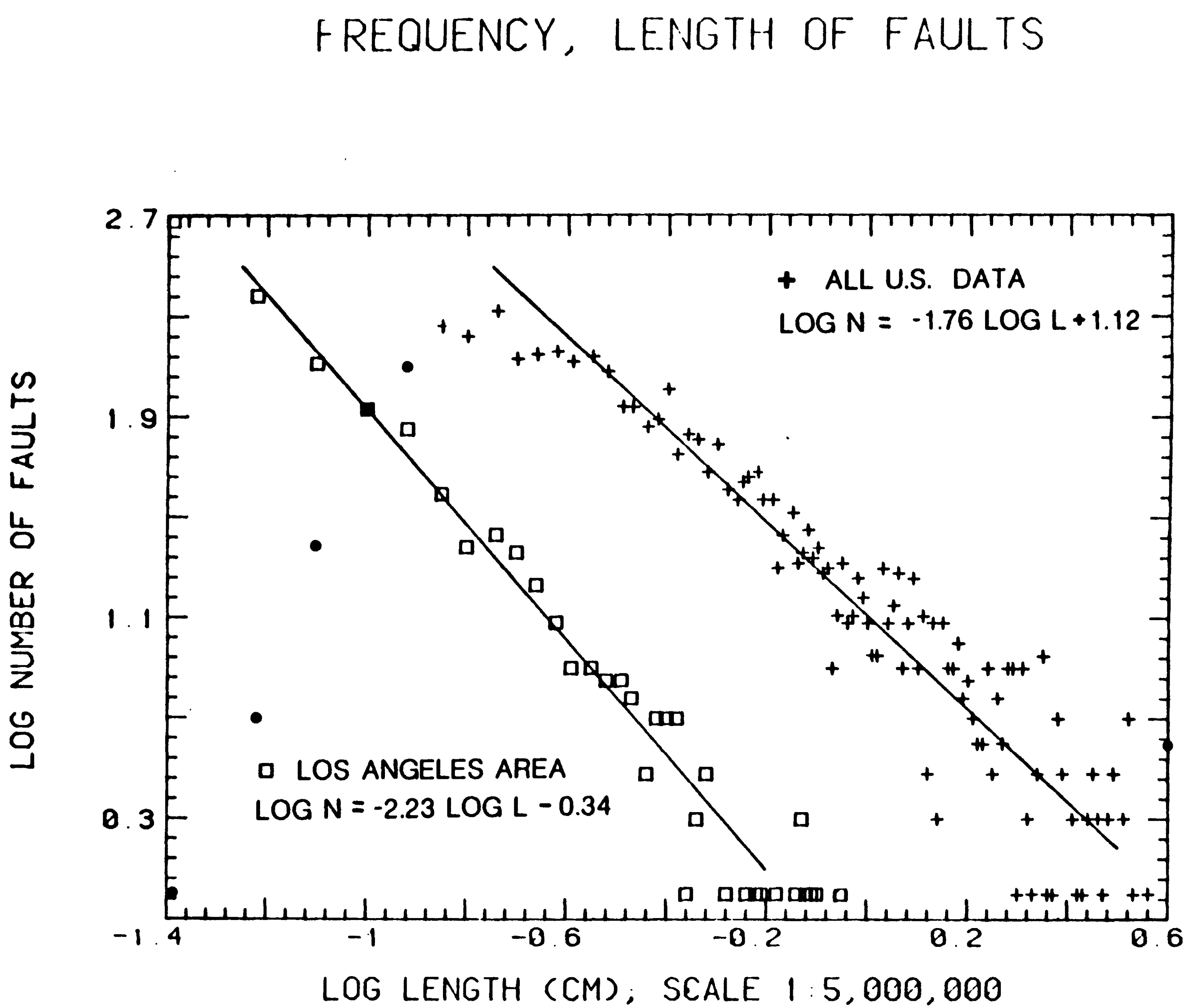

Figure 5. Comparisons of number frequencies versus lengths for all fault data from the conterminous U.S. and Los Angeles area respectively (modified from Shaw and others, 1981).
A. Log number versus log length for constant length intervals.

5A

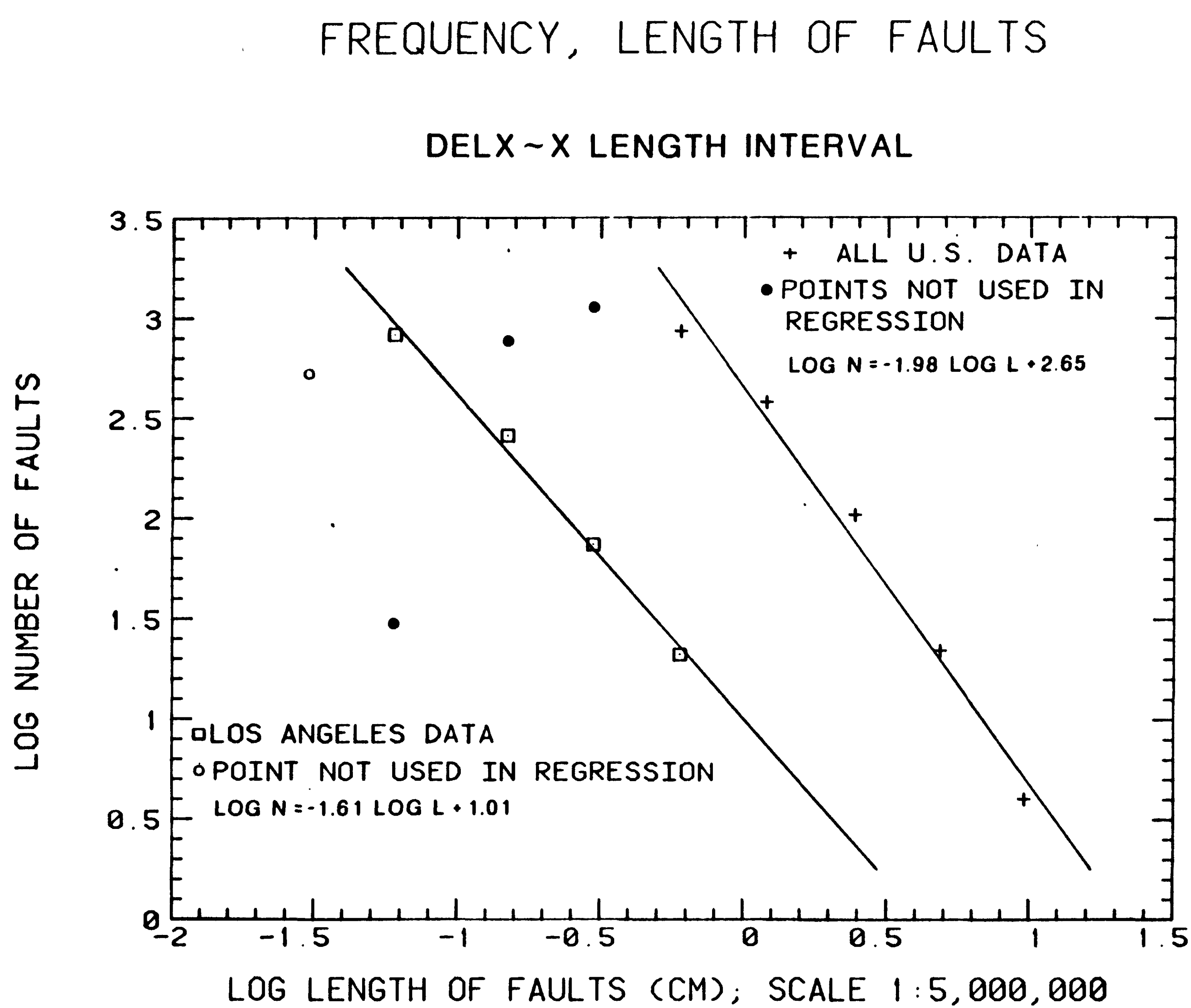

B. Log number versus log length for DELX~X.

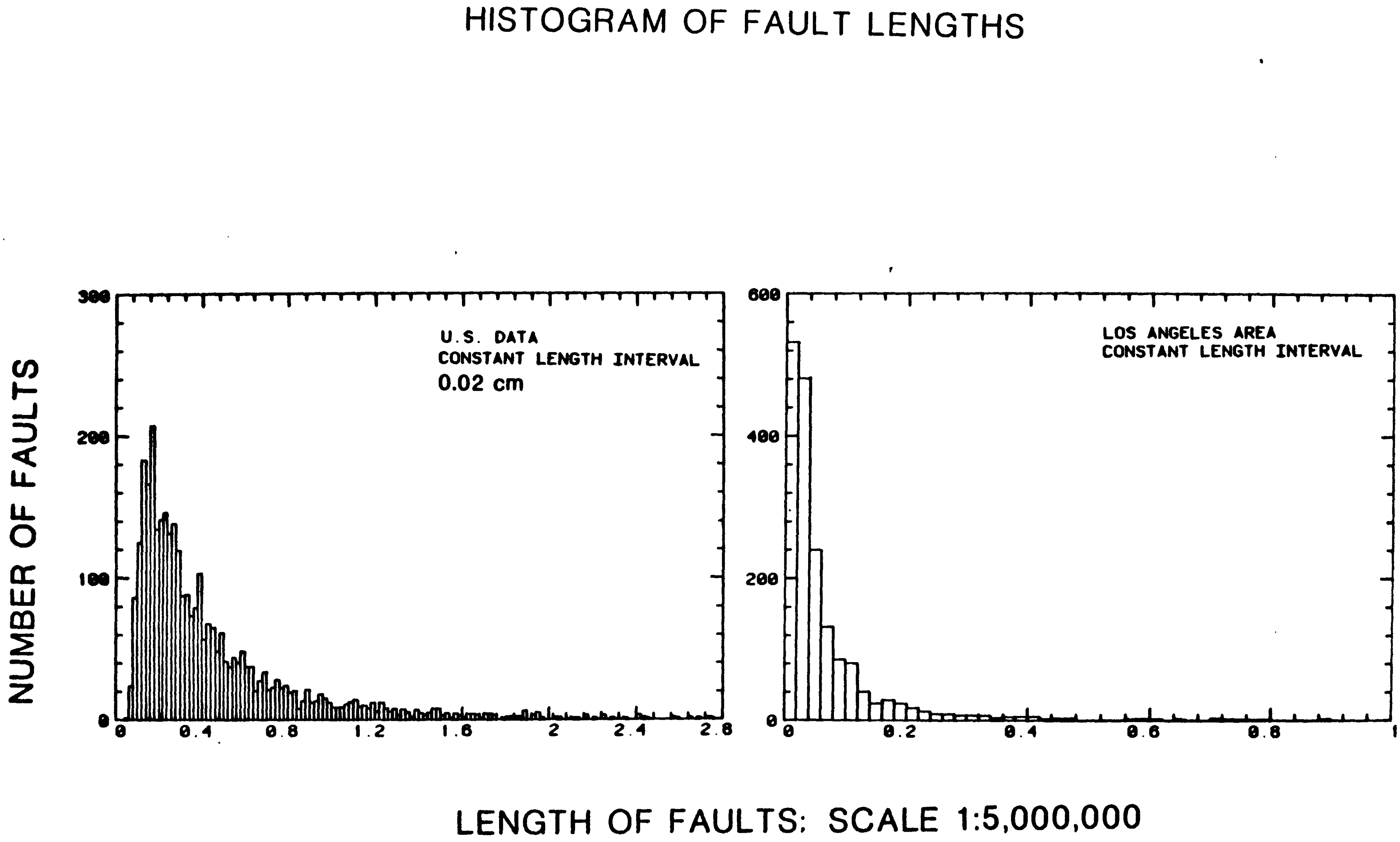

C. Histograms for constant length intervals.

5C

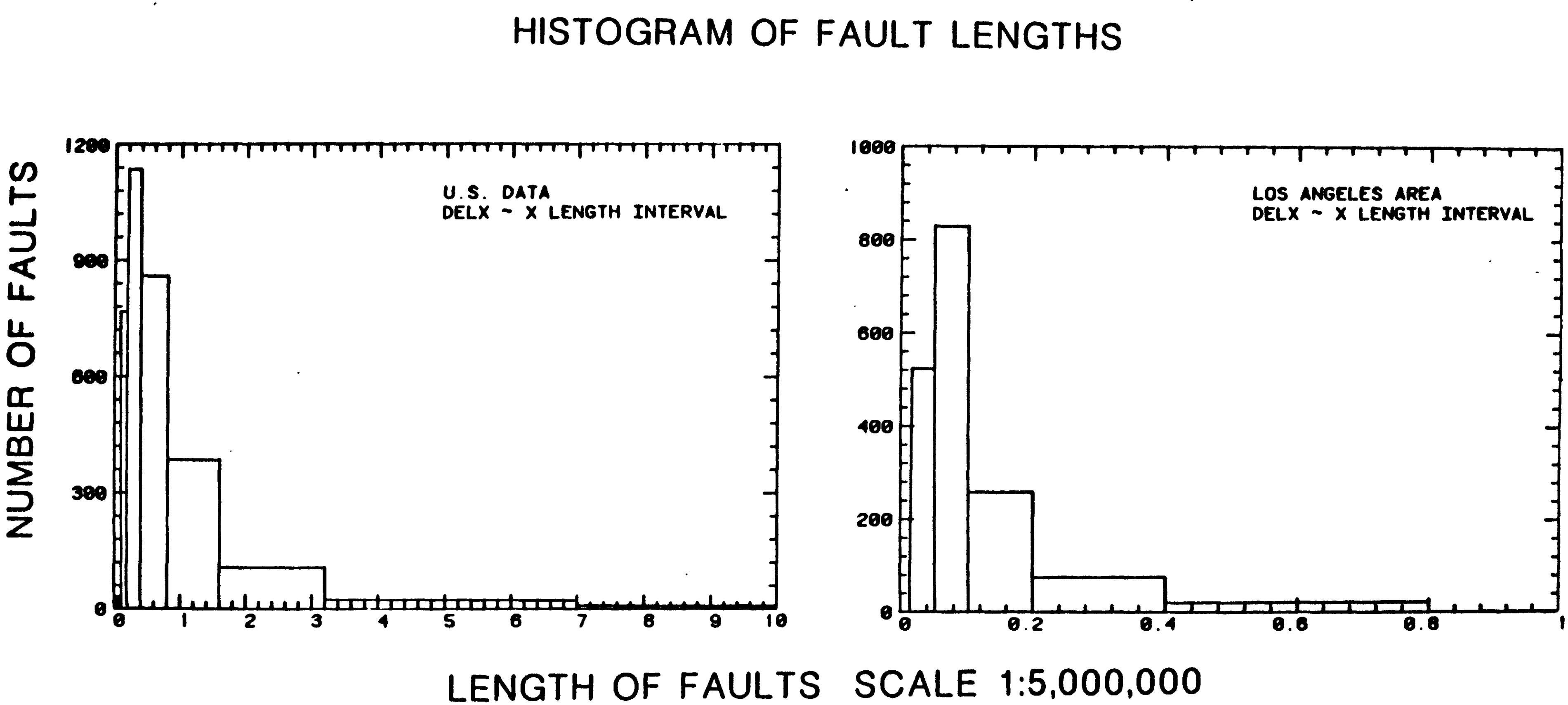

D. Histograms for DELX~X.

5D

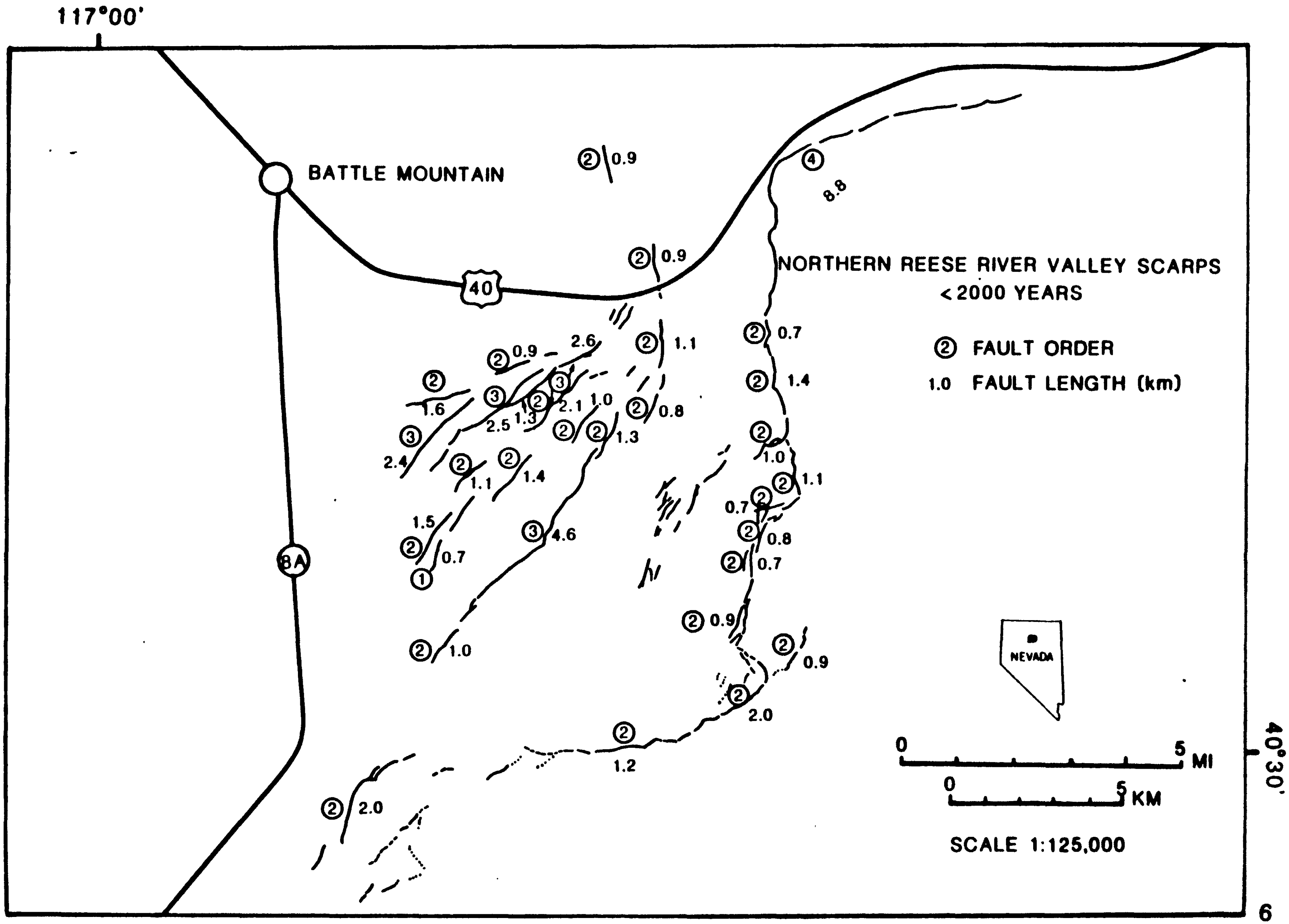

Figure 6. Fault map of the Northern Reese River Valley Scarps, Nevada (map pattern from Wallace, 1979). Fault segments are ordered in a manner analogous to ordering stream data, on the assumption that the dominant scarp in the northeast represents the highest order trunk fault. Segments not numbered are assumed to be order 1. Numerical data are given in Table 2 and in Figures 7 and 8.

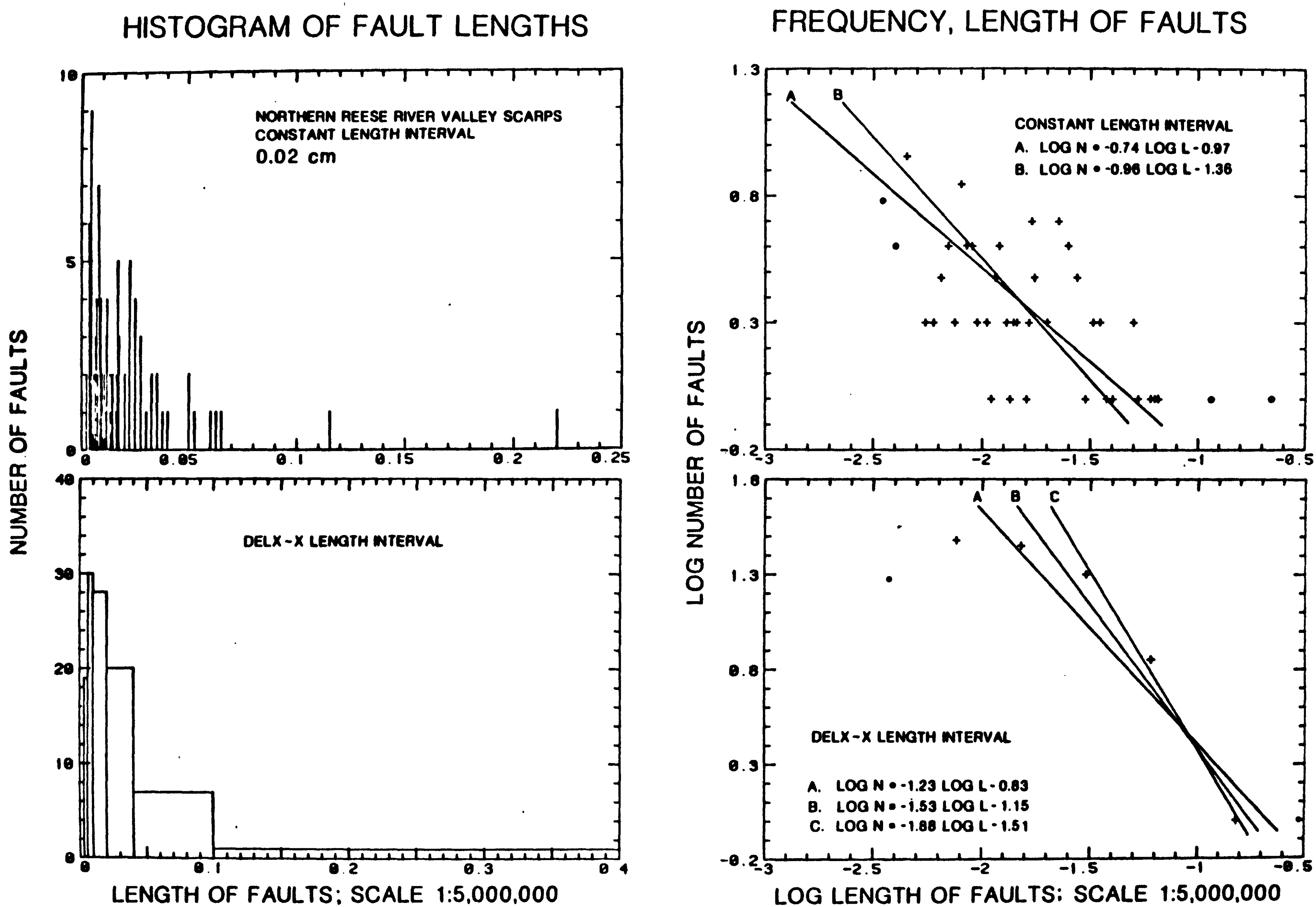

Figure 7. Histograms and regressions for number frequencies versus length for the Northern Reese River Valley Scarps compiled without regard to the classification by order in Figure 6.

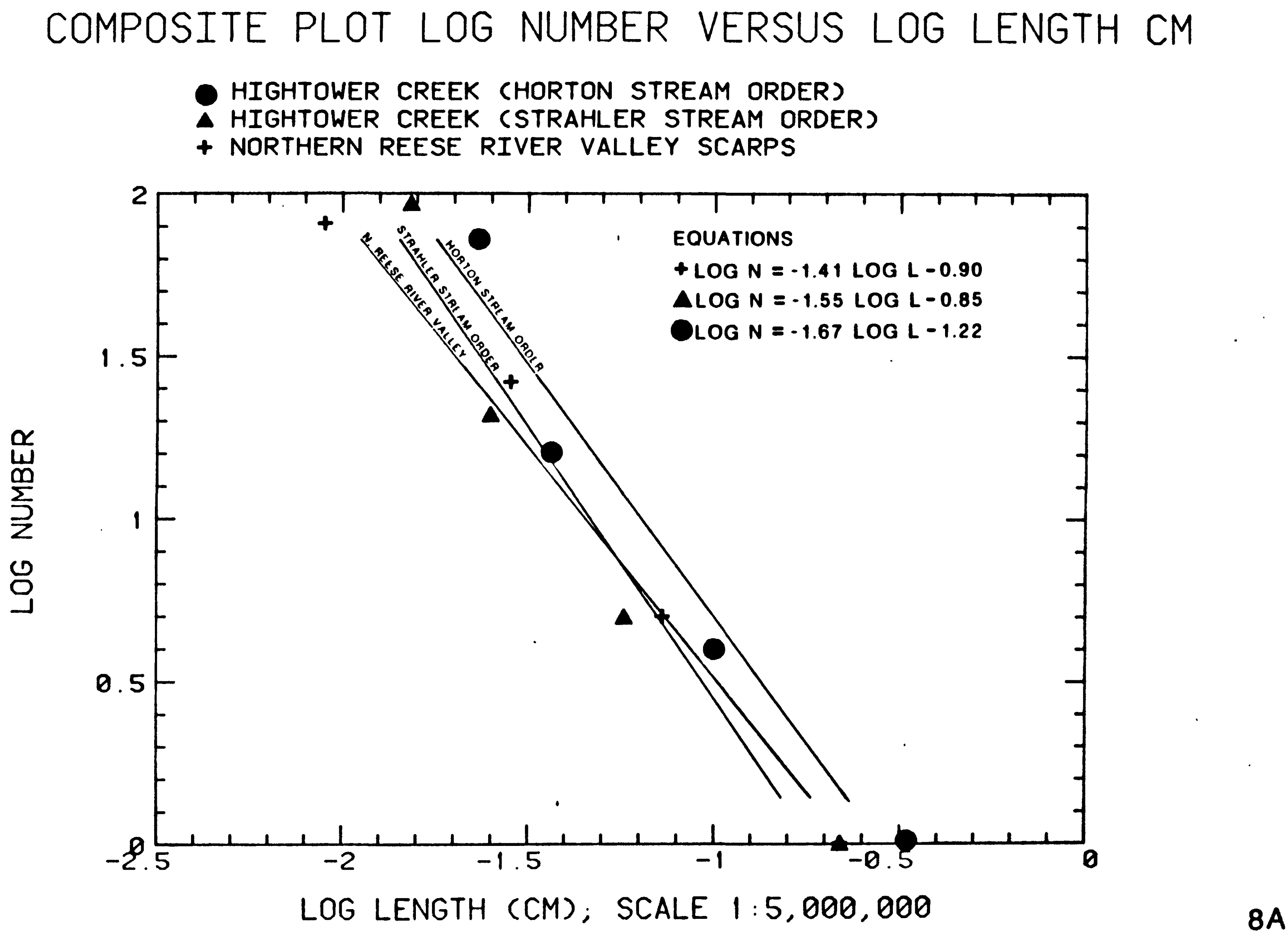

Figure 8. Data for number frequency versus mean length for Northern Reese River Valley Scarps ordered according to Figure 6 and compared with the ordered stream data for Hightower Creek from Figure 1A and Figure 2. A. Log number for each order versus log of mean length for each order.

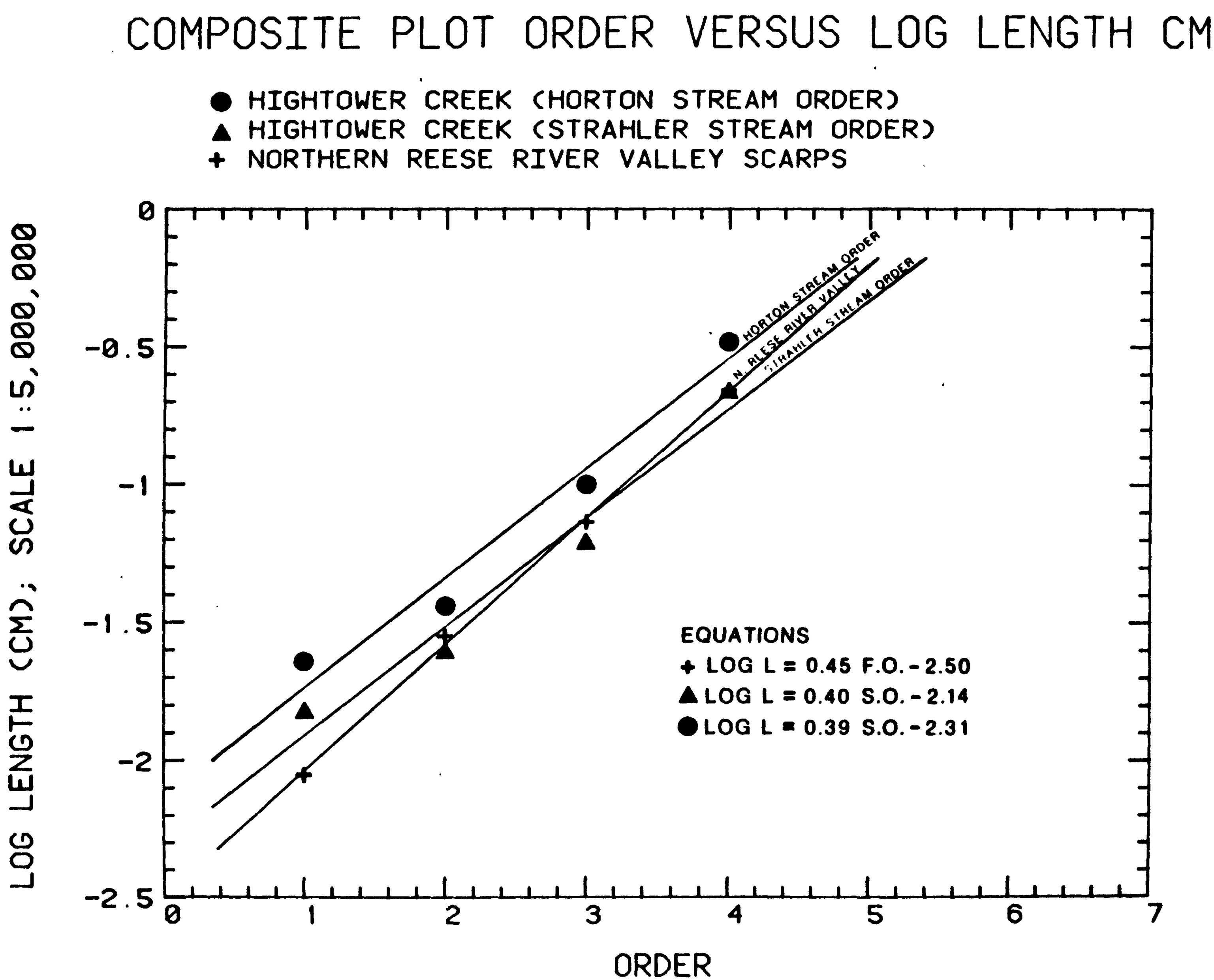

8. Log of mean length versus order.

8B

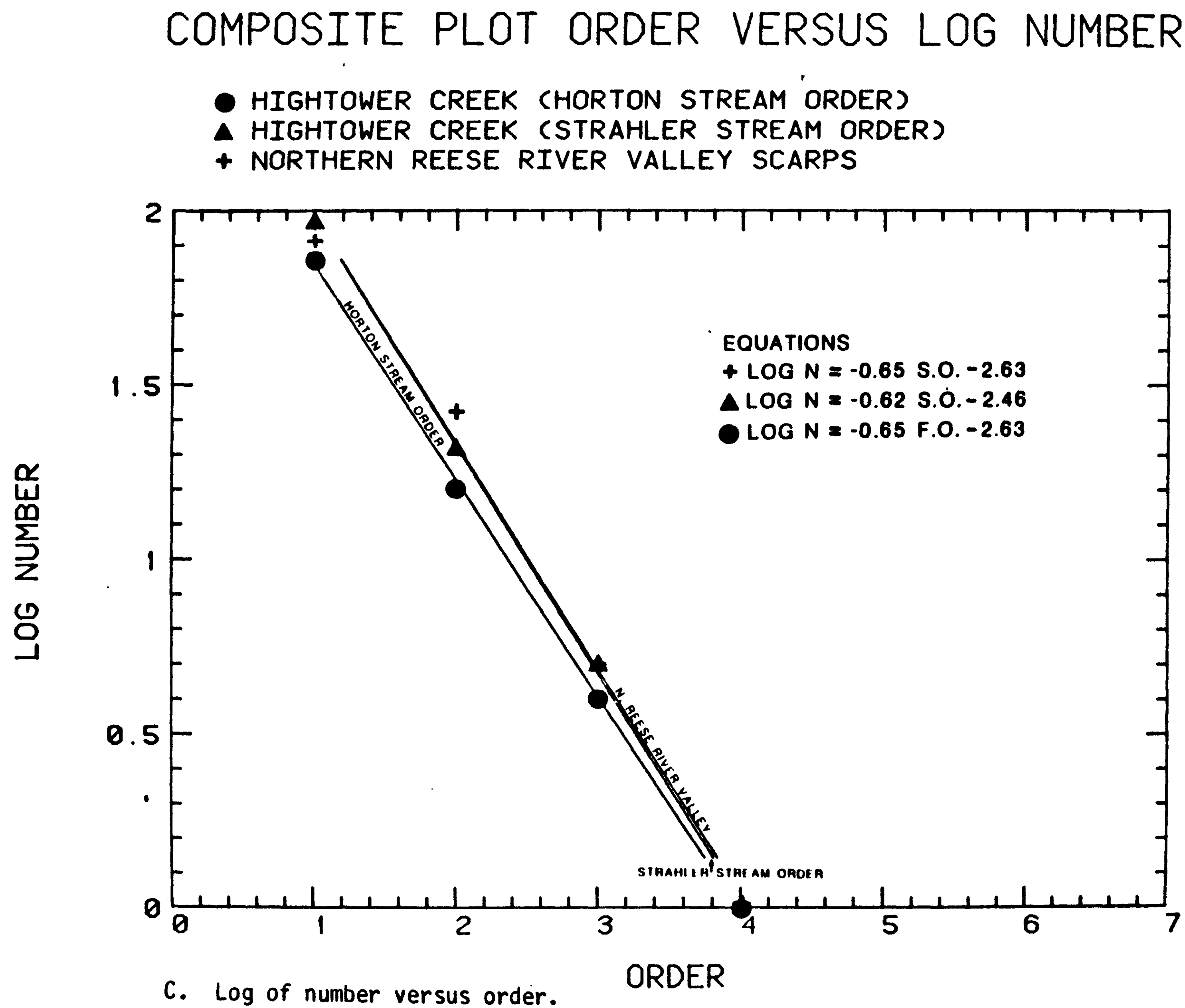

C. Log of number versus order.

8C

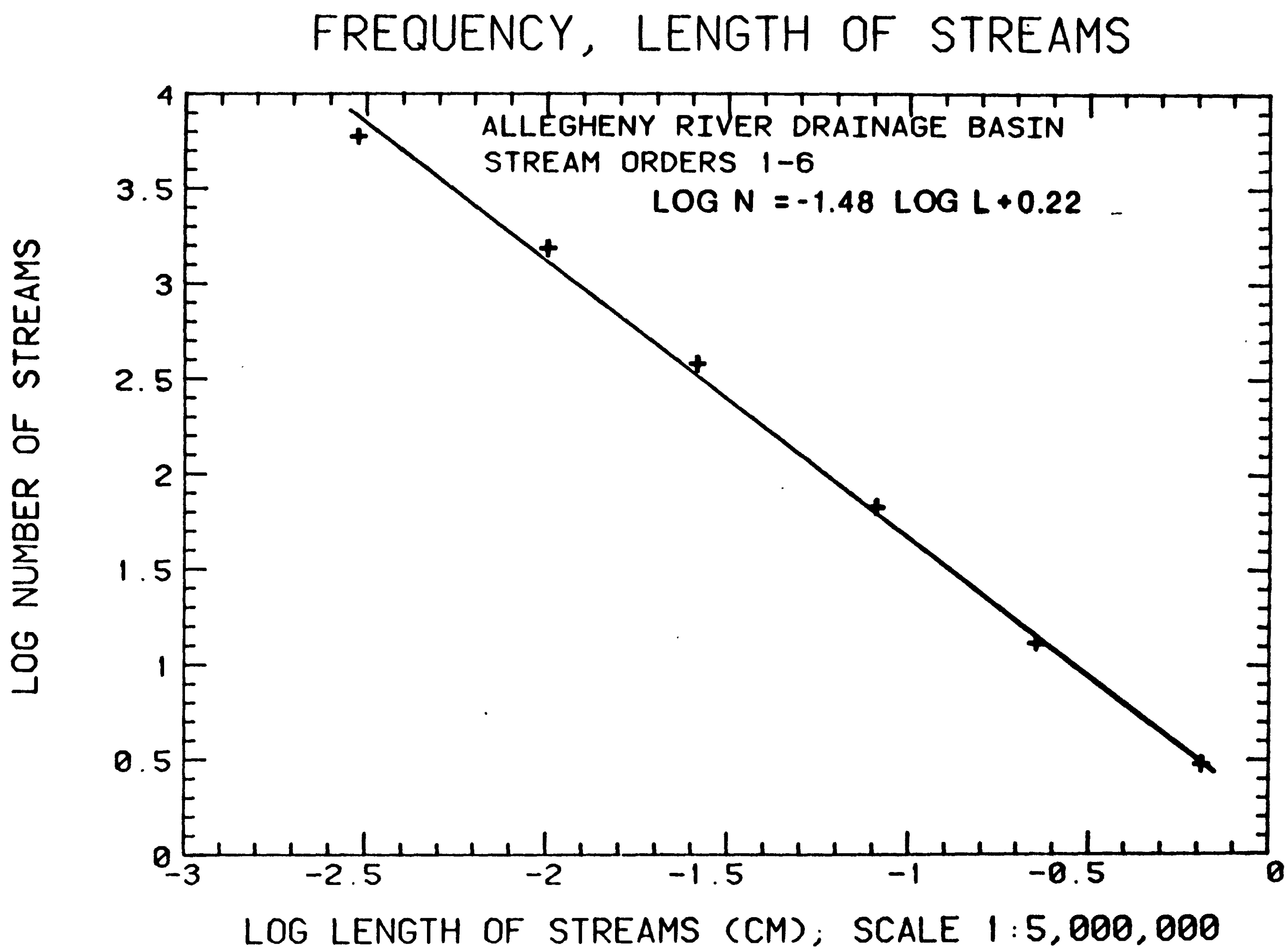

9A

Figure 9. Relations of stream orders, numbers and mean lengths for the Allegheny River system (data from Table 3).
A. Log number of streams per order versus log of mean length in each order.

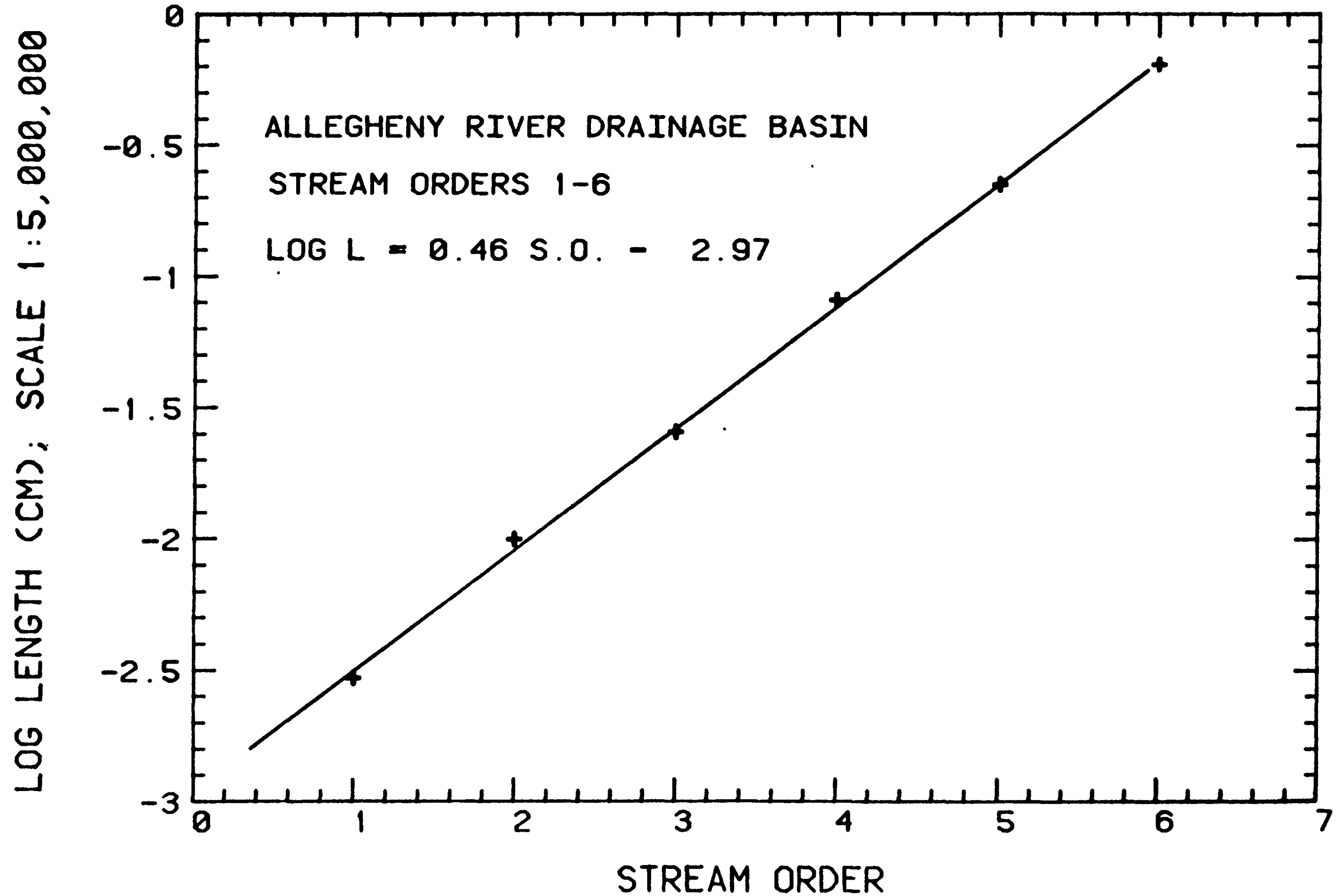

B. Log of mean length versus order.

9B

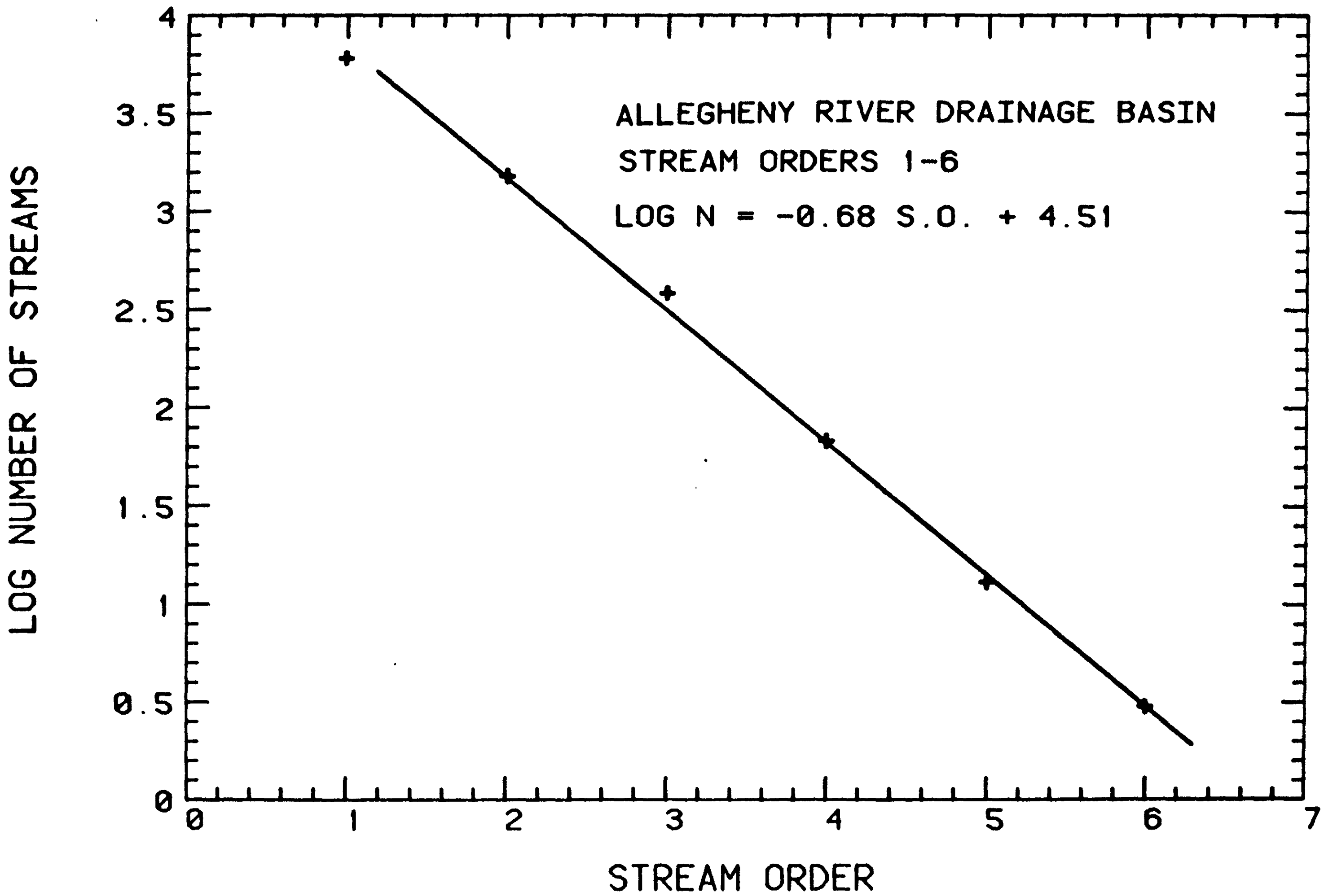

C. Log of number versus order.

9C

ORDER VERSUS LOG LENGTH; RIVER AND FAULT SYSTEMS

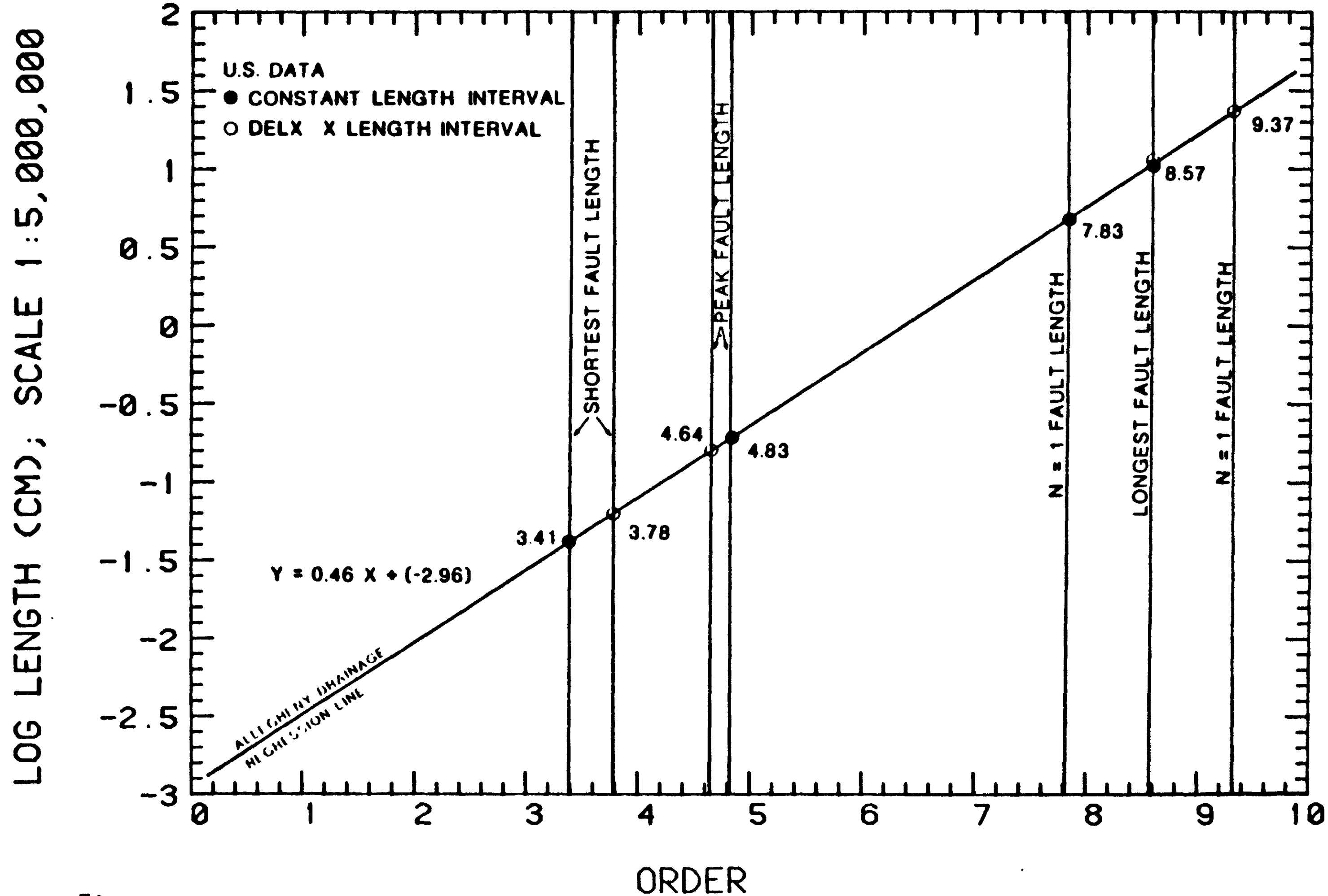

Figure 10. Length data for faults of the conterminous U.S. and L.A. area calibrated according to ordering relations for the Allegheny River system (Figure 9). Points indicate apparent order for fault systems at the shortest length represented by map data, the length at the maximum number frequency, the length at unit frequency from the regression equations (Figure 5) and the maximum map length, based on either the constant length or DELX~X conventions.

10A

ORDER VERSUS LOG LENGTH; RIVER AND FAULT SYSTEMS

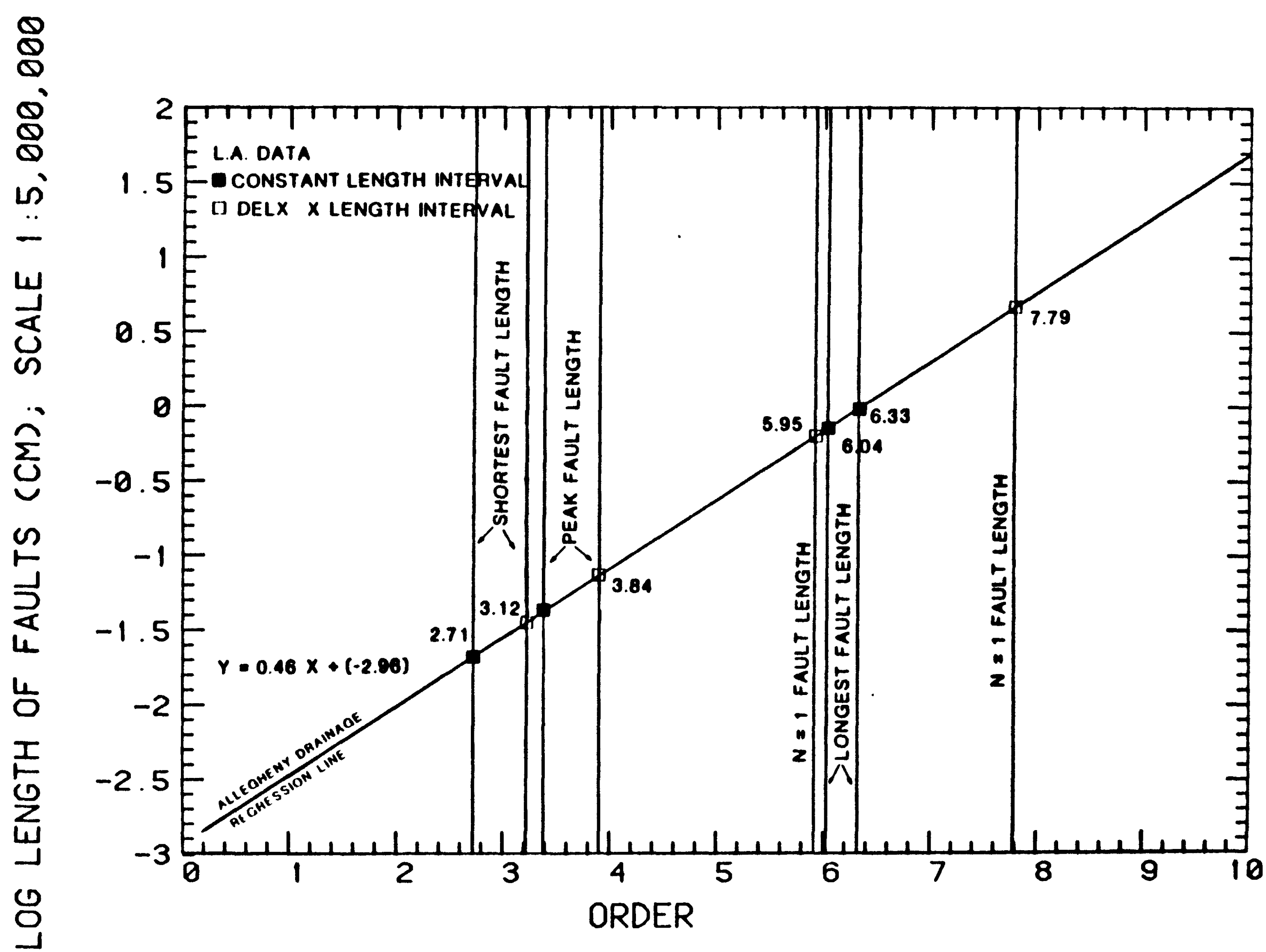

10B

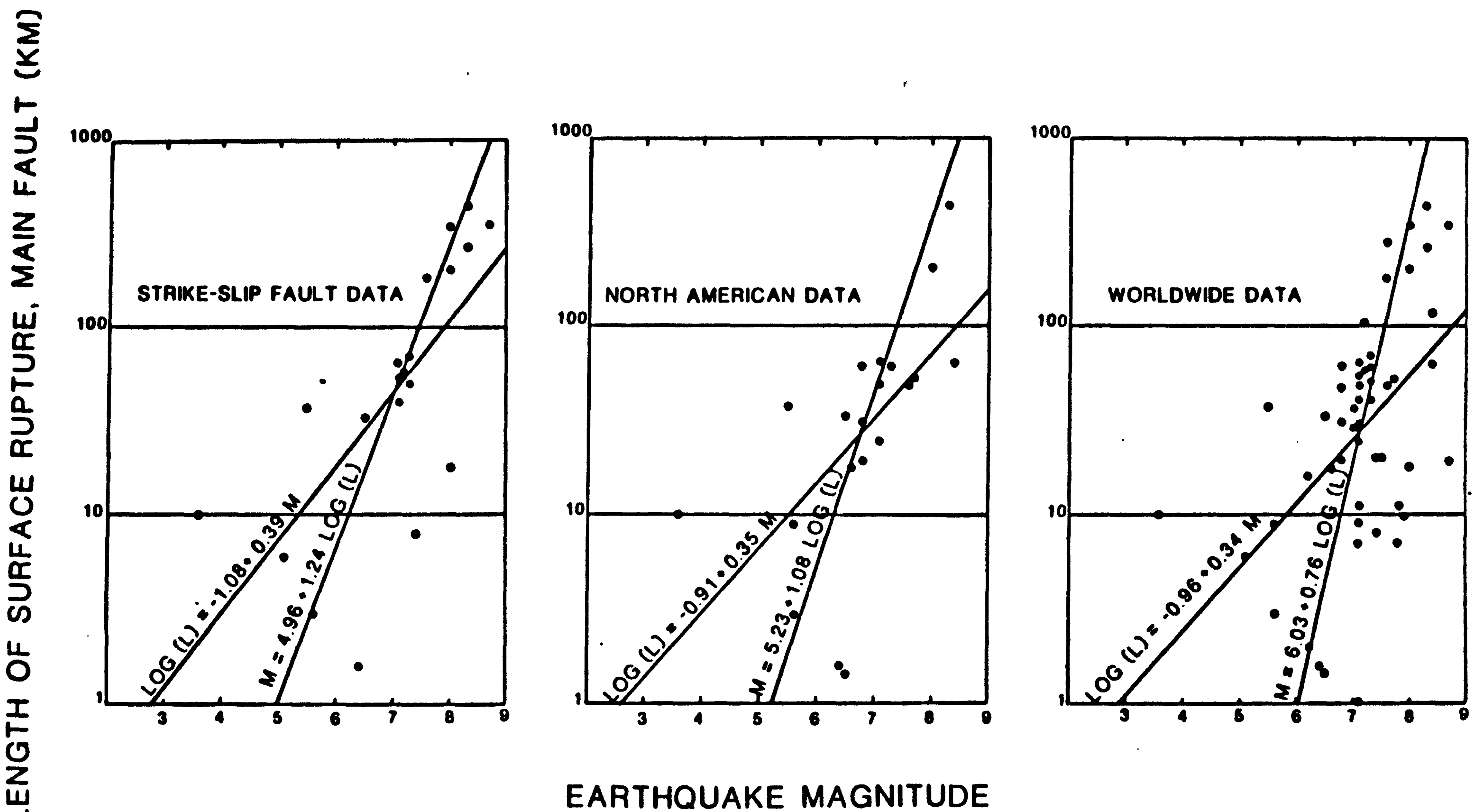

Figure 11. Data for log length versus earthquake magnitude with regressions of length on magnitude and magnitude on length (from Mark and Bonilla, 1977).

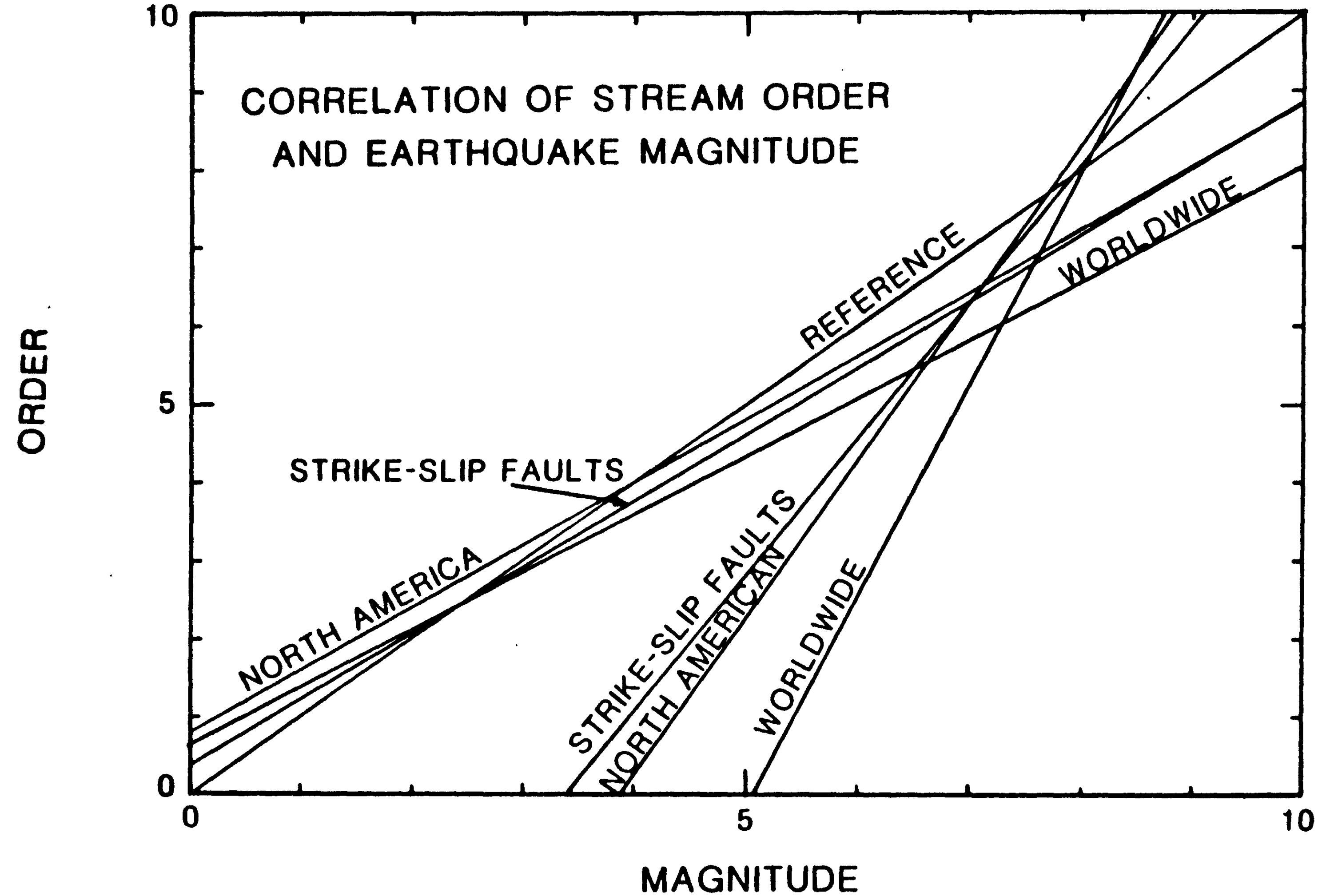

Figure 12. Correlations of fault order and earthquake magnitude using the Allegheny River system as reference for length versus order. A. The steeper set of curves are for magnitudes calculated from length according to Mark and Bonilla (1977) plotted versus order for that length. The set of lines having slopes near unity are for lengths calculated from magnitudes according to Mark and Bonilla (1977) and plotted at the order represented by that length from the Allegheny calibration of length versus order (Figure 9).

12A

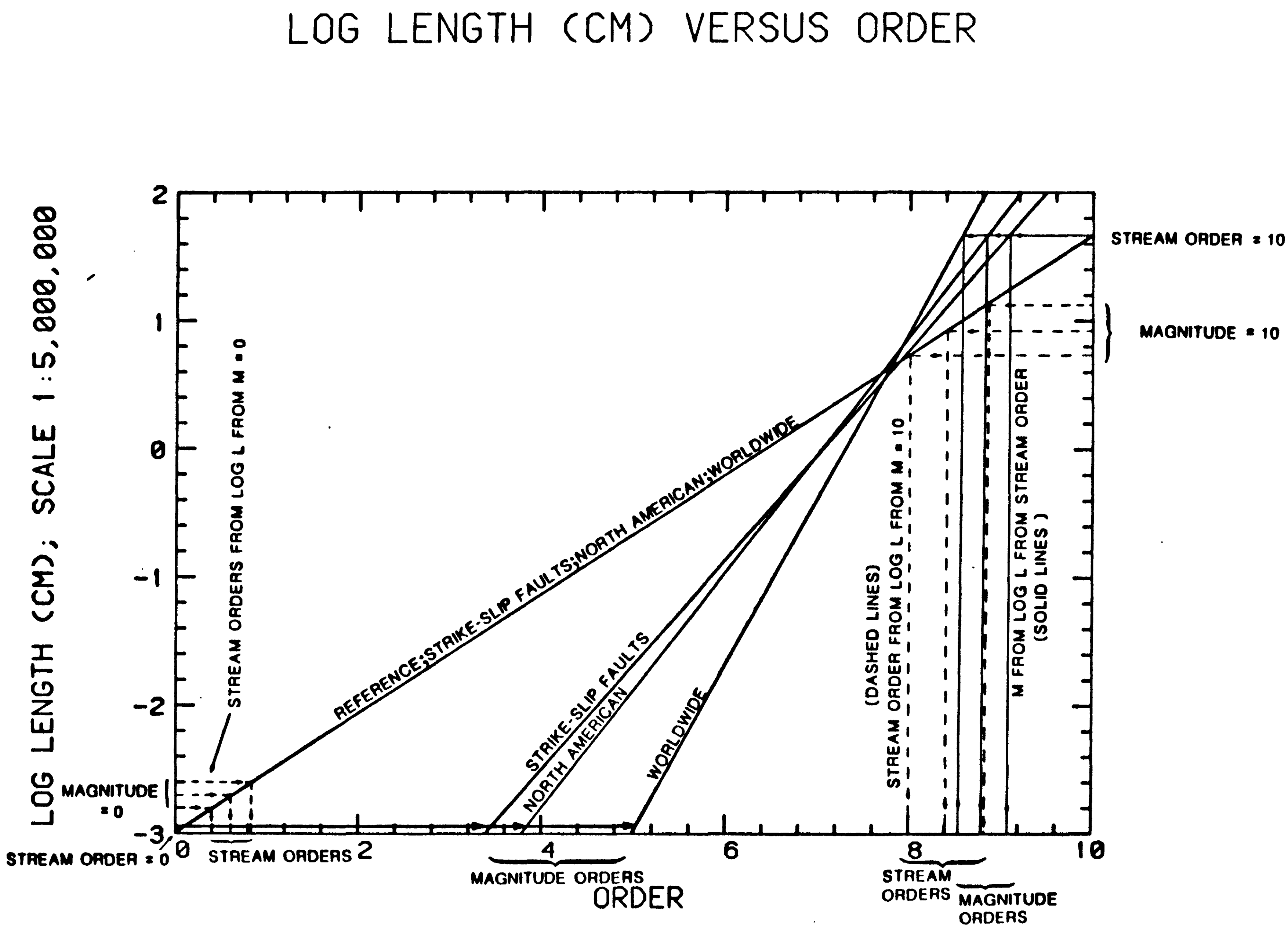

B. Relations in A represented as a plot of log length versus order and magnitude. Relations depend on whether the path of calculation is: stream order based on log length derived from earthquake magnitude; or, magnitude based on log length derived from stream order. In the former case the points plot along the reference curve of log length versus order for the Allegheny system of Figure 9.

12B

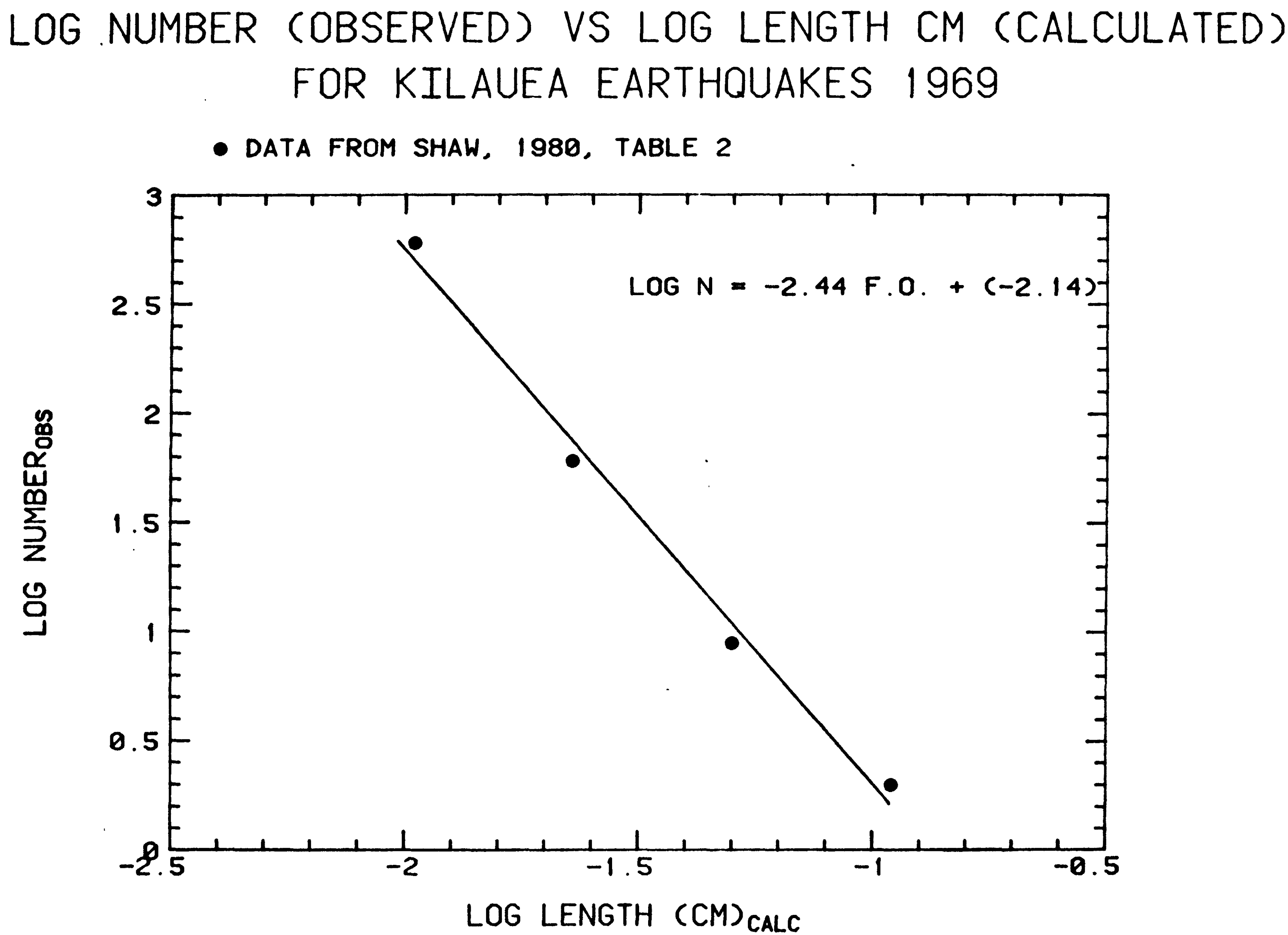

13A

Figre 13. Earthquake data for Kilauea volcano, 1969, ordered according to lengths calculated from magnitude (Mark and Bonilla, 1977, worldwide data); order calibrated according to Allegheny system (Figure 9).
A. Log of observed number versus log of mean length calculated from observed magnitude.

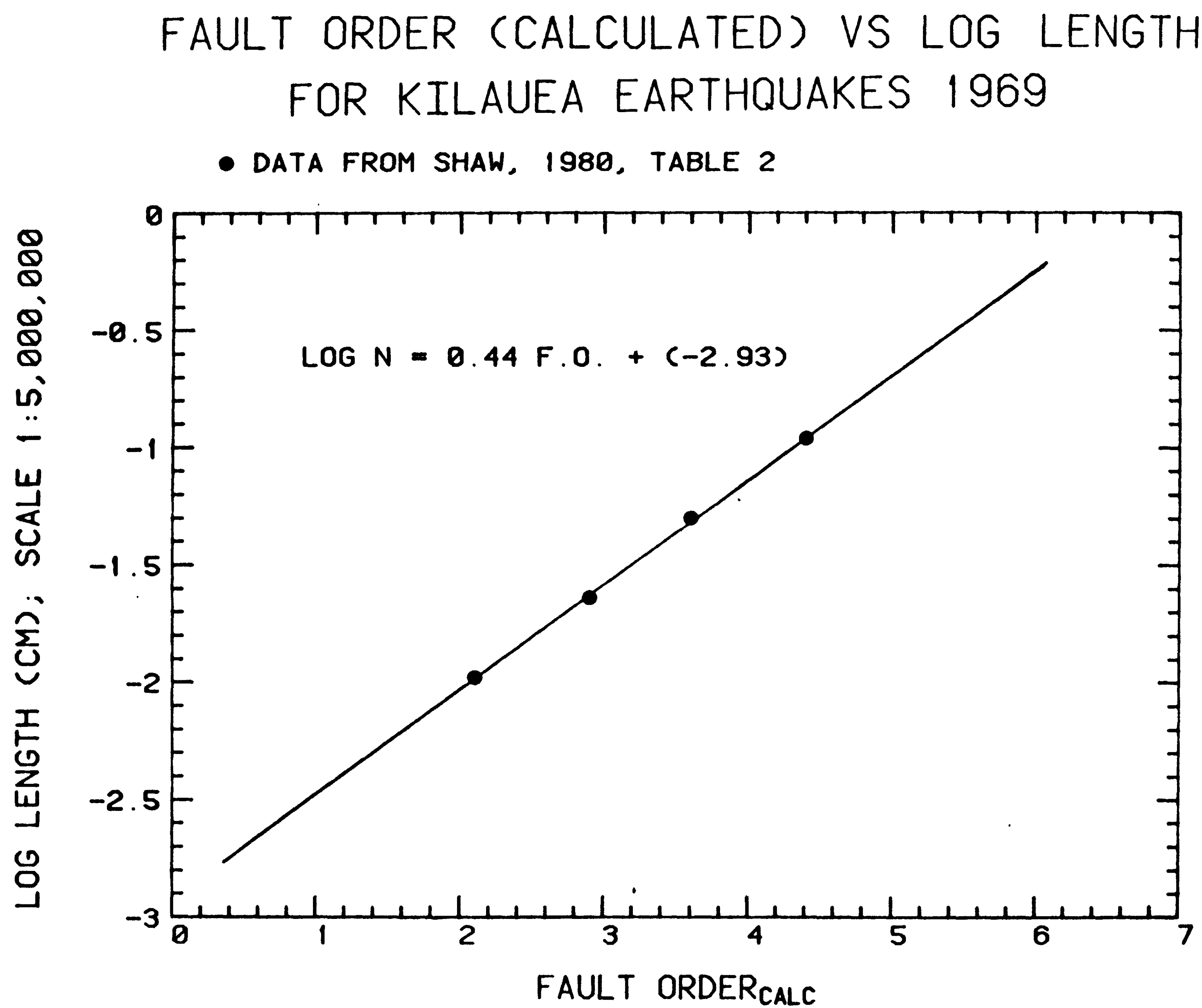

13B

B. Log of calculated lengths versus order calibrated from Allegheny system.

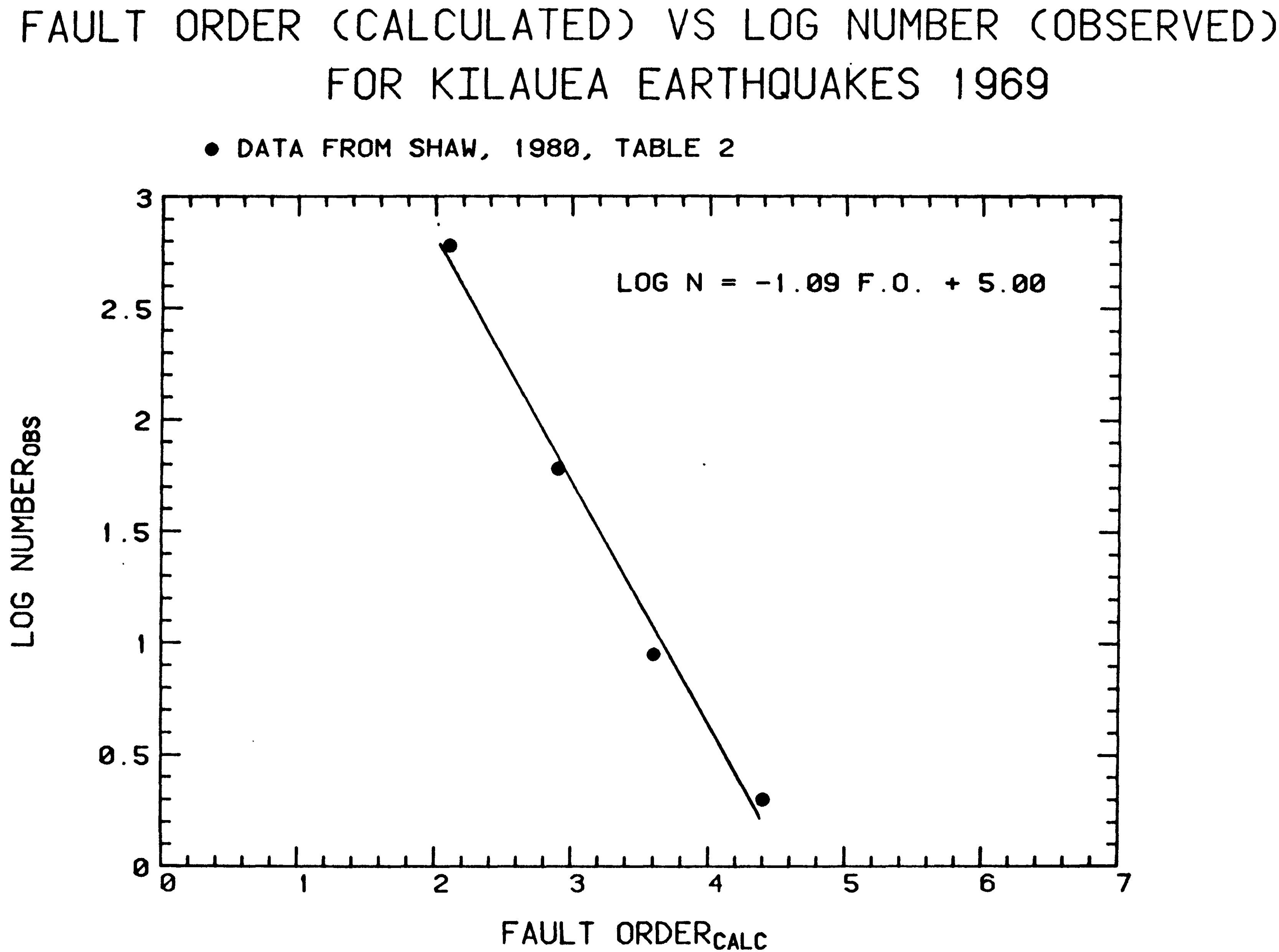

13C

C. Log of observed number versus fault order calibrated from calculated lengths in A (Allegheny Reference).

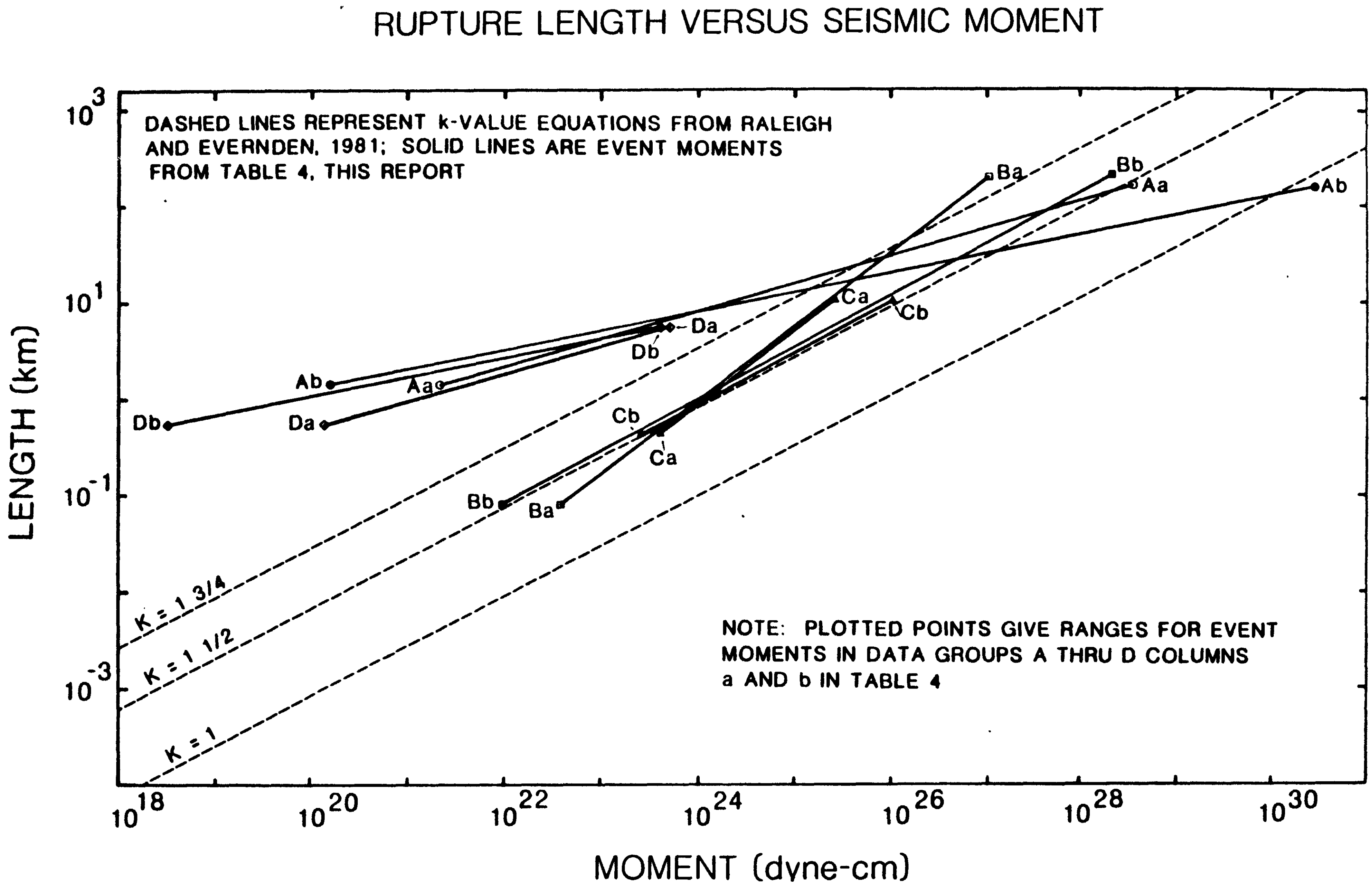

Figure 14. Correlations of apparent seismic moments and rupture lengths for different relations among rupture length, magnitude and moment in Table 4. Reference curves are from Raleigh and Evernden (1981). The divergent trends and apparent K ranges appear to depend on whether data are based on fault rupture lengths or magnitudes in Table 4; the former correspond more closely to the control curves, whereas the latter diverge to apparently high K values at the smaller moments. There apparently is a fundamental distinction between the length versus moment and magnitude versus moment relations.

14